R. & M. No. 2996
(14,734 and 15,629)
A.R.C. Technical Report

MINISTRY OF SUPPLY

AERONAUTICAL RESEARCH COUNCIL
REPORTS AND MEMORANDA

Low-Speed Tunnel Tests of Some Split Flap Arrangements on a 48-deg Delta Wing
Parts I and II

Part I

By

The Tunnel Staff

Part II

By

J. F. HOLFORD, B.A., and J. W. LEATHERS

LONDON: HER MAJESTY'S STATIONERY OFFICE
1957
NINE SHILLINGS NET

Low-Speed Tunnel Tests of Some Split Flap Arrangements on a 48-deg Delta Wing Parts I and II

Part I

By

The Tunnel Staff

Part II

By

J. F. Holford, B.A., and J. W. Leathers

Communicated by the Principal Director of Scientific Research (Air), Ministry of Supply

Reports and Memoranda No. 2996*

September, 1952

Summary.—The report is in two parts, following a general introduction. In Part I the effects of solid and vented flaps at various positions on a delta wing have been measured, and a drag coefficient found which uses an 'effective area' to cover the effect of venting (Fig. 15). A method of estimating the flap drag is given for this wing thickness and delta angle (Fig. 17).

It is shown that equal upper- and lower-surface flaps can cause a breakdown in the lift similar to that previously found on unswept wings[1,2], but the area in which this occurs is not likely to be used when such flaps are used as air brakes (Fig. 14).

In Part II the effects of lower-surface split flaps in various chordwise and spanwise positions on a delta wing have been measured for a range of flap deflections.

The results show that for small flap angles a type of flow exists in which the flow re-attaches to the wing surface behind the flap, causing zero or negative flap lift increments and positive pitching moments. Transition to this type of flow depends on the ratio of the height of the flap trailing edge off the wing surface to its distance ahead of the wing trailing edge, and also on the flap aspect ratio.

General Introduction.—A series of low-speed wind-tunnel tests have been made to investigate the behaviour of split flaps on one or both surfaces of a delta wing. The investigation is split into two parts described separately in the body of the report. Part I deals mainly with the estimation of the drag of such flaps with special reference to their use as air brakes on aircraft. Part II deals with an investigation into the phenomena of flow re-attachment behind the flaps and its effect on the flap characteristics.

PART I

The Drag of Brake Flaps on a Delta Wing

1. *Introduction*.—A study has been made in the past of the effect of brake flaps on unswept wings[1,2]. It was found that the drag could be predicted if the wing thickness and fore-and-aft position of the flap were included in the variables. It was also found that when equal upper

* R.A.E. Tech. Note Aero. 2124, received 18th March, 1952.
R.A.E. Tech. Note Aero. 2188, received 12th February, 1953.

and lower surface flaps of chord $0 \cdot 1c$ were placed at $0 \cdot 3c$ from the leading edge, a breakdown of the flow occurred, such that at a positive angle of incidence the lift coefficient was even less than it would have been with upper-surface brake flaps only[2], and the flow was very unsteady.

Tests have now been made using a 10 per cent thick delta wing with the leading edge swept back 48 deg, to find the drag of brake flaps in various positions, and to look for any positions to be avoided as causing a breakdown in the flow similar in type to that previously found.

The main results are:

(*a*) A coefficient is defined which takes account of venting between the brake flap and wing surface by giving an equivalent flap area (Fig. 15)

(*b*) In terms of this coefficient it is shown that the variations of drag coefficient with flap chord or span or spanwise position are small when tested on a delta wing without body (Fig. 7)

(*c*) The drag is a function of fore-and-aft position relative to the centre-line chord, and this function is different when the body, or ducts, etc., modify the pressure distribution on the wing (Fig. 17). These variations in drag will be less on a thinner wing since they arise from the pressure field due to thickness

(*d*) An area is defined inside which equal upper and lower surface brake flaps may cause a breakdown in the lift curve. This appears to involve a relationship between the size of the brake flap and its distance from the trailing edge of the delta, so that the dangerous area for a small chord flap is further to the rear than for a larger chord flap (Fig. 14).

2. *Model*.—The wing and flaps are shown in Fig. 1 and Table 1. The wing is of RAE 101 section (10 per cent thick with its maximum thickness at $0 \cdot 3c$). The flap chords were approximately 4 and 8 per cent c, where c is the centre-line chord, and the general layout of the tests is most easily seen from Fig. 2. All the flaps shown were tested at no lift, and those tested over an incidence range are marked. In Fig. 13 some additional flap positions are shown, used to determine the area of flow breakdown more exactly. The flaps were set at 60 deg in all cases, with hinges on the lines shown. The 'vented' flaps have the same solid part as the 'solid' flaps, but are carried at a distance from the wing surface leaving a constant gap of one-third of the smaller flap chord (or one-sixth of the larger).

The drag differences due to adding flaps to the wing are expressed as coefficients C_F, using a flap area S_F. In the case of vented flaps, the effective area is determined by adding $0 \cdot 55$ times the gap area to the solid area. This rough rule is only correct for small gaps, and the question of a more general coefficient is further discussed in section 5 for larger gaps.

3. *Results at* $C_L = 0$.—The flap drag coefficients C_F are tabulated in Figs. 3 and 4, the change of no-lift angle in Fig. 5, and the change of pitching moments in Fig. 6. Some anomalous results may be noted in Figs. 5 and 6, but these are associated with the breakdown of flow mentioned above and will be discussed later.

The drag results show:

(*a*) The coefficient used brings the solid and vented flap drags into good agreement

(*b*) The drag of flaps of different chord is proportional to S_F

(*c*) The drag coefficient of flaps of the same chord is reduced slightly by increasing the flap span, this effect being less when the flaps are vented (Fig. 7)

(*d*) The drag varies with fore-and-aft position of the flaps relative to the centre-line chord. The mean value of this variation is shown in Fig. 17.

4. *Results over C_L Range.*—4.1. *Drag.*—Fig. 8 shows the increase of drag with incidence for an upper surface flap, and decrease for a lower surface flap: the drag for equal flaps on both surfaces is also shown, and remains nearly constant. It will be seen that the same curves are obtained for small and large chord, vented, and solid flaps, with the one exception that the drag of small solid flaps mounted near the trailing edge on the upper surface of the wing does not increase much with increasing C_L. Since the flap chord was 4 per cent only of the root chord, this will be an effect of the thick boundary layer on the model at the low Reynolds number of the test.

4.2. *Lift.*—Figs. 9 to 12 show the changes in the lift due to flaps. From Figs. 9 and 10, upper-surface flaps are seen to displace the no lift angle, with little change in lift slope, while lower-surface flaps may reduce the slope. With equal upper- and lower-surface flaps (Figs. 11 and 12), the effect of flaps is normally to make no change in no-lift angle, but to reduce the lift slope slightly.

It is however obvious that at certain positions on the wing, a breakdown of flow is occurring, so that flaps on both surfaces may reduce the lift at a given incidence even more than similar upper-surface flaps used alone (*see* 2AB on Figs. 10 and 12 in position 2).

Extra flap positions were tested to define more precisely the area of flow breakdown (Fig. 13), and this area is shown in Fig. 14. It is seen that the distance from the trailing edge is doubled when the flap chord is doubled, so that it appears that a sufficiently long surface behind the flap can stabilise the flow. On this model, the worst breakdown occurs when the trailing edge is 5 flap chords behind the flap.

The effect on lift of venting the flaps is small, but in the case of flap 2AB (Fig. 12), venting reduces the suddenness of the change from one type of flow to the other, and provides a transition curve.

Some tests were made on a different wing of larger size to check the scale effect from 1 to 3×10^6. The effect of increased Reynolds number was similar to the effect of venting, it reduced the suddenness of the change in type of flow, but did not reduce the final loss of lift.

5. *Comparison of Present Results with Miscellaneous Brake Flap Tests on Delta Aircraft Models.*—To compare tests with different flap angle β, the coefficient C_F is divided by $\sin^2 \beta$. Since the gap between flap and wing is sometimes large, the method of allowing for gap is extended. With a large gap and small flap, the drag of the supports becomes appreciable, and the area of supports is added to the solid flap area. The results are replotted in this form, and show that for gaps larger than $0 \cdot 3$ times the flap chord, the drag is nearly constant at $1 \cdot 2$ times the drag of the flap with zero gap. Combining this with the previous rule of adding $0 \cdot 55$ times the area of small gaps to the solid area provides a definition of effective flap area, *i.e.*, effective flap area = solid flap area + support area + $0 \cdot 55 \times$ gap area, with the proviso that effective flap area is never greater than $1 \cdot 2$ times the solid flap + supports.

All the models compared have wings of 10 per cent thickness ratio with leading-edge sweepback between 45 deg and 53 deg, and the models are sketched in Fig. 16. The complete model results do not in general agree with the wing results (Fig. 17), having lower drag for forward flaps and higher for rear flaps. This is related to changes in pressure distribution caused by bodies and duct systems.

The jet bomber model with wing leading-edge entries has a more forward position of the wing thickness leading to a maximum suction line at $C_L = 0$ near the leading edge (*see* Figs. 16b and 16e). The flaps are located behind the position of the suction peak, instead of on it, as for the wing alone[8]. The resulting flap drag is lower than for the flap on the wing alone.

For flaps placed nearer the trailing edge, the effect of thickening the wing to enclose ducts increases the flap drag. In Fig. 16b, rear flaps are shown on two versions of a bomber model in which (*a*) the ducts are centrally placed relative to the wing chord, and (*b*) they are dropped so that they leave the upper surface of the wing nearly unaltered. These two cases are represented by open and closed circles in Fig. 17, where it will be seen that the drag of rear flaps in case (*b*) (closed circles) agrees with that of a flap on the wing alone, while the drag in case (*a*) is considerably higher. The effect of a body is less easy to estimate: the rear flaps on the jet fighter model have the higher drag value, whereas the slimmer body of a delta model tested at the National Physical Laboratory (Fig. 16d) does not alter the flap drag from the ' wing ' value.

The results of this survey are disappointing in that they do not provide a rule for estimating the drag of brake flaps on any delta aircraft: but they do give limits between which it is likely to lie for a 10 per cent wing of 50 deg leading-edge sweep, and some indication of how the drag varies with the pressure field. These variations will be less on a thinner wing.

One comparison between delta models with 45-deg. and 60-deg leading-edge sweep (Ref. 7) shows the flap drag coefficient to be 25 per cent less on the 60-deg delta.

6. *Conclusions.*—(*a*) A coefficient C_F is defined for expressing the drag of the brake flaps which takes account of the gap between the wing surface and the flap (Fig. 15). This coefficient is plotted for $\alpha = 0$ against position of the flap relative to the centre-line chord of a delta wing and various delta aircraft models all with 10 per cent thick wing section, in Fig. 17. The difference between the wing-alone results and those for the aircraft models is explained in a general way in terms of the changes in pressure distribution on the wing due to fuselage interference and to changes in wing thickness to accommodate ducts and jet pipes.

The drag of equal upper- and lower-surface flaps is little affected by incidence; the changes due to lift on the drag of single-surface flaps is shown in Fig. 8.

(*b*) Equal upper- and lower-surface flaps may cause a breakdown in flow if placed in the areas indicated in Fig. 14 (wing alone). These areas are not likely to be used in practice. Experiments should be made at higher Reynolds number if brake flaps are proposed which might cause such a breakdown of flow.

NOTATION

c	Wing centre-line chord
$\bar{c}$	Wing mean chord
c_F	Brake flap chord
b_F	Brake flap span
g	Gap between brake flap and wing in the plane of the flap
β	Brake flap angle of deflection
$\Delta\alpha$	Change in no-lift angle due to brake flaps
ΔC_{M0}	Change in pitching-moment coefficient due to brake flaps
ΔC_D	Change in drag at constant C_L due to brake flaps
C_F	Flap drag coefficient $= \Delta C_D \times S/S_F$

where S is the wing area

S_F is effective flap area

For solid flaps, S_F = flap area

For vented flaps, S_F = flap area + bracket area + $0\cdot55$ × gap area

with the proviso that effective flap area is never greater than $1\cdot2$ × area of solid flap + brackets.

REFERENCES

No.	Author	Title, etc.
1	Adamson	Brake flaps: recent wind-tunnel tests on a complete model and on rectangular wings fitted with brake flaps. R.A.E. Report Aero. 1685. June, 1941.
2	R. H. Whitby and F. J. Bigg ..	Wind-tunnel tests on the effect of brake flaps on lift and trim. R.A.E. Report Aero. 1744. A.R.C. 5860. March, 1942.
3	G. F. Moss	Measurements of aileron and elevator hinge moments on the Avro 707B with unbalanced and balanced controls. R.A.E. Tech. Note Aero. 2079. A.R.C. 13,905. October, 1950.
4	A. V. Roe Tunnel Staff ..	Wind-tunnel tests on the Avro 707. A. V. Roe W.T. Report WT/7/49. July, 1949.
5	J. Seddon, D. J. Kettle and J. Scanlon.	Low-speed tests on a 1/7 scale model of a twin-engined jet fighter with a delta wing. R.A.E. Report Aero. 2306. A.R.C. 12,247. December, 1948.
6	D. J. Kettle	Addendum to R.A.E. Report Aero. 2306. R.A.E. Report Aero. 2306a. A.R.C. 12,405. March, 1949.
7	R. Jones, C. J. W. Miles and P. S. Pusey.	Experiments in the Compressed Air Tunnel on swept-back wings, including two delta wings. R. & M. 2871. March, 1948.
8	D. J. Raney	Low-speed tunnel investigation of the pressure distribution over a delta wing of aspect ratio 3 at small incidences. R.A.E. Tech. Note Aero. 2062. A.R.C. 13,657. July, 1950.

TABLE 1

Details of Delta Wing and Brake Flaps

All linear dimensions given as a percentage of the wing centre-line chord c.

$c = 19 \cdot 0$ in.

Wing	
Area	$0 \cdot 889c^2$
Span	164·2
Mean chord	54·2
Aspect ratio	3·03
Section	RAE 101 (symmetrical)
Thickness	10 per cent at 31 per cent chord
Sweepback of leading edge	48 deg
Dihedral	0 deg
Geometric twist	0 deg
Wing quarter-chord point (pitching moments referred to this point)	
Distance aft of leading edge at centre-line of model	49·8
Brake flaps	
Chord	3·95; 7·89
Span	15·8; 31·6· 47·4
Deflection	60 deg
Gap between flap and wing in the plane of the flap with vented flaps	1·32
Each flap secured to the wing by two brackets each of width	1·32

TABLE 1—*continued*

Details of Delta Wing and Brake Flaps

Brake flap positions on wing

Flap Symbol	Flap Span	Wing chord at flap centre-line	Spanwise position (Distance of flap from model centre-line)	Chordwise position Distance of flap hinge from:	
				(*a*) leading edge at wing centre-line	(*b*) local leading edge (per cent local chord)
(*a*) Basic flap positions					
1A	15·8	79·4	18·4	39·5	23·8
2A	15·8	79·4	18·4	60·5	50·3
2B	15·8	61·8	34·2	60·5	36·1
3A	15·8	79·4	18·4	81·6	76·8
3B	15·8	61·8	34·2	81·6	70·2
3C	15·8	44·1	50·0	81·6	58·3
2AB	31·6	70·5	26·3	60·5	43·8
3AB	31·6	70·5	26·3	81·6	73·9
3ABC	47·4	61·8	34·2	81·6	70·2
(*b*) Additional flap positions used for investigation of breakdown of flow					
D	15·8	79·4	18·4	31·6	13·9
E	15·8	73·5	23·7	39·5	17·7
F	15·8	73·5	23·7	44·7	24·8
G	15·8	79·4	18·4	52·6	40·4
H	15·8	67·6	28·9	52·6	30·0
J	31·6	100·0	0	60·5	60·5
K	15·8	70·5	26·3	60·5	44·1
L	15·8	52·9	42·1	60·5	25·4
M	15·8	79·4	18·4	68·4	60·2
N	15·8	52·9	42·1	68·4	40·0

TABLE 2

Lift, Drag and Pitching Moment without Flaps

$R = 1{\cdot}0 \times 10^6$

α	C_L	C_D	C_m
0	0	0·0087	0
3·4	0·176	0·0130	−0·0170
7·0	0·351	0·0253	−0·0326
10·3	0·512	0·0521	−0·0419
14·2	0·663	0·1008	—

TABLE 3

Lift; Drag due to Flaps

$R = 1 \cdot 0 \times 10^6$

(a) Solid flaps. Lower surface

α	C_L	ΔC_D	C_F	α	C_L	ΔC_D	C_F
1A–S				2A–S			
−10·7	−0·498	0·0284	2·025	− 7·4	−0·342	0·0190	1·355
− 7·3	−0·336	0·0238	1·695	− 3·7	−0·167	0·0187	1·33
− 3·9	−0·160	0·0196	1·395	− 0·2	0	0·0171	1·22
− 0·4	0	0·0165	1·175	+ 3·2	+0·163	0·0155	1·105
+ 3·2	+0·171	0·0139	0·99	+ 6·7	+0·325	0·0140	0·995
6·9	0·338	0·0120	0·855				
10·4	0·503	0·0096	0·685				
+13·8	+0·648	0·0107	0·76				
3A–S				1A–L			
−11·9	−0·513	0·0147	1·045	− 7·1	−0·322	0·0462	1·645
− 8·5	−0·339	0·0127	0·905	− 3·7	−0·160	0·0389	1·385
− 4·6	−0·150	0·0129	0·92	− 0·1	−0·001	0·0330	1·175
− 1·1	+0·001	0·0125	0·89	+ 3·5	+0·161	0·0282	1·005
+ 2·6	0·189	0·0127	0·905	5·8	0·269	0·0260	0·925
6·2	0·354	0·0110	0·785	10·6	0·486	0·0211	0·75
9·8	0·515	0·0074	0·525	+14·1	+0·633	0·0232	0·825
+13·2	+0·651	0·0068	0·485				
2A–L				3A–L			
−11·7	−0·497	0·0435	1·55	−13·2	−0·523	0·0354	1·26
− 7·9	−0·330	0·0400	1·425	− 9·6	−0·355	0·0286	1·02
− 4·7	−0·155	0·0378	1·345	− 6·0	−0·170	0·0264	0·94
− 1·2	0	0·0344	1·225	− 2·2	+0·002	0·0249	0·885
+ 2·4	+0·148	0·0316	1·125	+ 1·3	0·179	0·0236	0·84
6·0	0·296	0·0290	1·035	4·9	0·349	0·0216	0·77
9·4	0·445	0·0276	0·985	8·5	0·511	0·0146	0·52
+13·1	+0·577	0·0348	1·24	+11·8	+0·658	0·0051	0·18
3C–L				2AB–L			
−13·0	−0·523	0·0334	1·19	−11·6	−0·284	0·0771	1·37
− 9·5	−0·344	0·0303	1·08	− 8·3	−0·128	0·0710	1·265
− 5·7	−0·168	0·0282	1·005	− 4·9	0	0·0652	1·16
− 2·3	0	0·0260	0·925	− 1·3	+0·122	0·0606	1·08
+ 1·2	+0·168	0·0243	0·865	+ 2·1	0·239	0·0562	1·00
4·8	0·329	0·0215	0·765	5·4	0·353	0·0514	0·915
8·2	0·485	0·0189	0·675	+ 8·8	+0·460	0·0511	0·91
+11·6	+0·618	0·0203	0·725				
3AB–L				3ABC–L			
−15·6	−0·544	0·0694	1·235	−17·9	−0·562	0·1071	1·275
−12·0	−0·363	0·0536	0·955	−14·2	−0·405	0·0742	0·885
− 8·3	−0·183	0·0466	0·83	−10·3	−0·191	0·0641	0·765
− 4·6	0	0·0452	0·805	− 6·7	−0·003	0·0652	0·775
− 1·0	+0·164	0·0442	0·785	− 3·0	+0·158	0·0645	0·77
+ 2·6	0·327	0·0417	0·74	+ 0·4	0·319	0·0625	0·745
6·2	0·490	0·0334	0·595	3·8	0·468	0·0560	0·665
+ 9·7	+0·642	0·0181	0·32	+ 7·3	+0·614	0·0441	0·525

(4966) A**

TABLE 3—*continued*

Lift; Drag due to Flaps

(*b*) *Vented flaps. Lower surface*

α	C_L	ΔC_D	C_F	α	C_L	ΔC_D	C_F
3A–S				1A–L			
−12·4	−0·515	0·0225	1·355	−10·8	−0·463	0·0579	1·89
− 8·8	−0·350	0·0179	1·075	− 7·4	−0·316	0·0490	1·60
− 5·3	−0·176	0·0165	0·99	− 3·9	−0·154	0·0418	1·365
− 1·6	0	0·0155	0·93	− 0·2	0	0·0354	1·155
+ 1·9	+0·159	0·0148	0·89	+ 3·2	+0·156	0·0315	1·025
5·5	0·327	0·0140	0·84	6·8	0·316	0·0276	0·90
9·0	0·490	0·0100	0·60	10·3	0·476	0·0242	0·79
+12·5	+0·636	0·0078	0·47	+13·8	+0·621	0·0279	0·91
2A–L				3A–L			
−11·6	−0·475	0·0503	1·64	−13·3	−0·516	0·0418	1·365
− 8·3	−0·317	0·0437	1·425	− 9·6	−0·346	0·0326	1·065
− 4·9	−0·145	0·0401	1·31	− 6·0	−0·158	0·0287	0·935
− 1·2	−0·001	0·0369	1·205	− 2·5	+0·002	0·0264	0·86
+ 2·2	+0·150	0·0338	1·10	+ 1·2	0·174	0·0254	0·83
5·5	0·301	0·0309	1·01	4·7	0·343	0·0231	0·755
9·0	0·446	0·0288	0·94	8·1	0·505	0·0164	0·535
+12·6	+0·579	0·0332	1·085	+11·9	+0·653	0·0080	0·26
2AB–L				3AB–L			
−14·4	−0·395	0·0999	1·63	−16·0	−0·521	0·0838	1·365
−10·9	−0·242	0·0828	1·35	−12·4	−0·357	0·0638	1·04
− 7·5	−0·109	0·0752	1·225	− 8·8	−0·183	0·0553	0·90
− 4·1	0	0·0704	1·15	− 5·1	0	0·0506	0·825
− 0·6	+0·132	0·0651	1·06	− 1·5	+0·153	0·0476	0·775
+ 2·8	0·262	0·0588	0·96	+ 2·1	0·316	0·0465	0·76
6·1	0·387	0·0542	0·885	5·6	0·475	0·0379	0·62
+ 9·5	+0·514	0·0531	0·865	+ 9·1	+0·629	0·0231	0·375
3ABC–L							
−14·4	−0·387	0·0818	0·89				
−10·7	−0·181	0·0759	0·825				
− 7·0	−0·001	0·0737	0·80				
− 3·4	+0·147	0·0711	0·775				
0	0·305	0·0696	0·755				
+ 3·5	0·453	0·0627	0·68				
+ 6·9	+0·600	0·0495	0·54				

TABLE 3—*continued*

Lift; Drag due to Flaps

(*c*) *Solid flaps. Both surfaces*

α	C_L	ΔC_D	C_F	α	C_L	ΔC_D	C_F
1A–S				2A–S			
0	0	0·0343	1·22	0	0	0·0327	1·165
3·3	0·165	0·0348	1·24	3·5	0·161	0·0326	1·16
6·5	0·323	0·0362	1·29	6·8	0·317	0·0316	1·125
2B–S				3A–S			
0	0	0·0368	1·31	0	0	0·0272	0·97
3·4	0·152	0·0374	1·33	3·1	0·162	0·0267	0·95
6·4	0·304	0·0381	1·355	6·8	0·336	0·0254	0·905
3C–S				2AB–S			
0	0	0·0290	1·035	0	0	0·0740	1·32
2·1	0·014			2·9	0·006	0·0718	1·28
3·8	0·095			6·3	0·145	0·0723	1·29
5·7	0·178			3AB–S			
7·6	0·257			0	0	0·0510	0·91
				3·6	0·152	0·0499	0·89
				6·7	0·311	0·0484	0·86
1A–L				2A–L			
0	0	0·0707	1·26	0	0	0·0696	1·24
3·4	0·149	0·0722	1·285	2·7	0·095	0·0690	1·23
6·8	0·292	0·0758	1·35	6·4	0·254	0·0688	1·225
10·0	0·452			9·7	0·387	0·0695	1·24
				13·1	0·520		
2B–L				3A–L			
0	0	0·0743	1·325	0	0	0·0503	0·895
1·8	−0·004			3·6	0·167	0·0515	0·915
4·0	0·028			7·2	0·347	0·0505	0·90
6·1	0·113			10·7	0·501	0·0511	0·91
7·3	0·207			13·9	0·621	0·0544	0·97
10·2	0·342						
12·7	0·478						
3C–L				2AB–L			
0	0	0·0523	0·93	0	0	0·1442	1·285
2·1	0·073	0·0527	0·94	1·8	+0·062		
3·4	0·126	0·0535	0·955	3·0	+0·092	0·1430	1·27
6·7	0·305	0·0555	0·99	4·8	−0·092		
10·2	0·446			6·5	−0·030	0·1299	1·155
				8·1	+0·041		
				11·3	+0·182		
				14·2	+0·325		
3AB–L							
0	0	0·0983	0·875				
3·5	0·144	0·0973	0·865				
7·0	0·288	0·0973	0·865				

TABLE 3—*continued*

Lift; Drag due to Flaps

(*d*) *Vented flaps. Both surfaces*

α	C_L	ΔC_D	C_F	α	C_L	ΔC_D	C_F
1A–L				2AB–L			
0	0	0·0767	1·25	0	0		
3·1	0·137	0·0778	1·27	2·0	−0·010		
6·5	0·275	0·0819	1·335	2·9	−0·007		
				3·8	−0·018		
2A–L				5·4	+0·005		
0	0	0·0736	1·20	7·1	0·039		
2·7	0·098	0·0737	1·20	8·6	0·087		
5·1	0·151			11·1	+0·176		
6·6	0·213	0·0752	1·225				
7·7	0·249			2B–L			
9·8	0·368			0	0	0·0768	1·25
12·6	0·494			3·1	0·018	0·0758	1·235
				6·5	0·151	0·0778	1·27
3A–L				9·6	0·293	0·0823	1·34
0	0	0·0579	0·945	12·5	0·445		
2·8	0·111	0·0579	0·945				
6·9	0·271	0·0594	0·97				

TABLE 4

Pitching Moment; Flaps on Both Surfaces

C_L	C_m	C_L	C_m
3C–S (Solid)		2AB–L (Vented)	
0	0	0	0
0·014	0·0308	0·018	+0·0184
0·095	0·0264	0·151	+0·0033
0·178	0·0208	0·293	−0·0178
0·257	0·0183		

TABLE 5

Extra Flap Positions (D to N) on Both Surfaces : Lift

$R = 0{\cdot}67 \times 10^6$

Flap chord = 7·89 per cent c; flap span = 15·8 per cent c

α	C_L						
	Flap positions :—						
	D	E	F	F*	G	H
0	0	0	0	0	0	0
2·5	0·128	0·122	0·110	0·100	0·092	0·081
5·0	0·246	0·238	0·220	0·204	0·182	0·157
7·5	0·361	0·357	0·335	0·293	0·310	0·262
10·0	0·471	0·467	0·452	0·408	0·420	0·403
12·5				0·499		

α	Flap positions :— J	K	L	M	N
0	0	0	0	0	0
2·5	−0·024	0·043	−0·048	0·105	−0·040
5·0	+0·088	0·130	+0·050	0·204	+0·053
7·5	0·201	0·252	0·162	0·316	0·174
10·0	0·327	0·382	0·285	0·404	0·300
12·5	0·431		0·480		0·423
15·0	0·548		0·595		+0·550
17·5			+0·701		

α	Flap positions 2B (Upper) K (Lower)	2B (Upper) 2A (Lower)
0	0	0
2·5	0·028	0·061
5·0	0·108	0·146
7·5	0·228	0·260
10·0	0·364	

* Vented flaps.

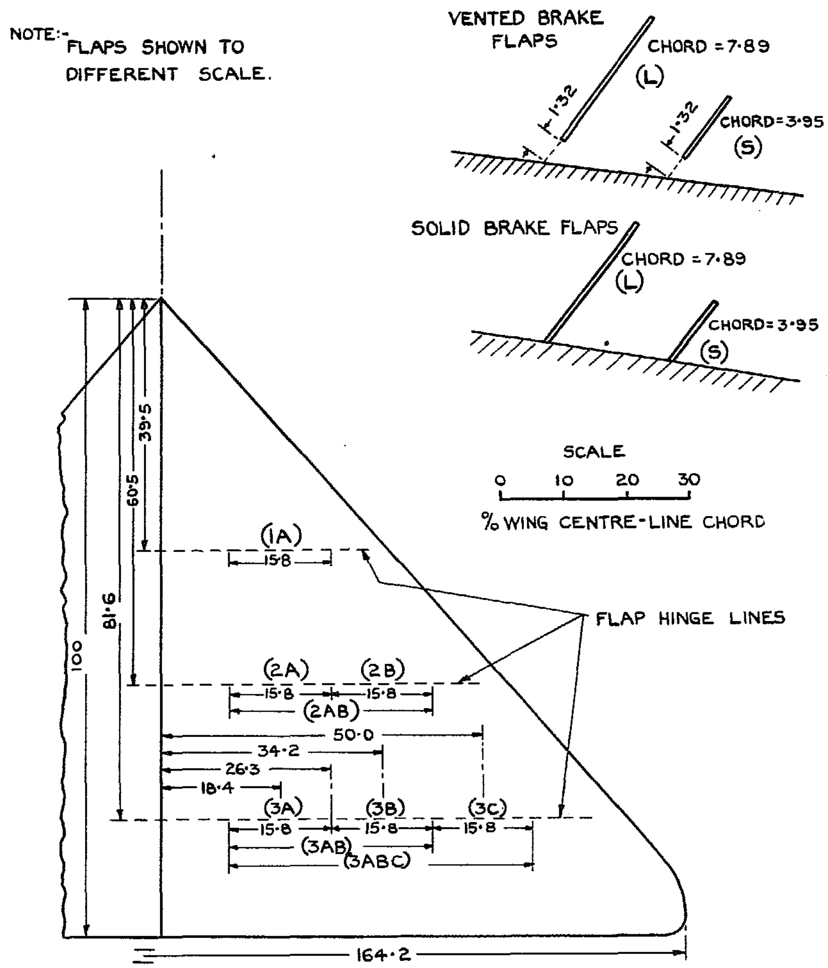

DIMENSIONS GIVEN AS PERCENT WING CENTRE-LINE CHORD.

FIG. 1. Wing and brake flaps.

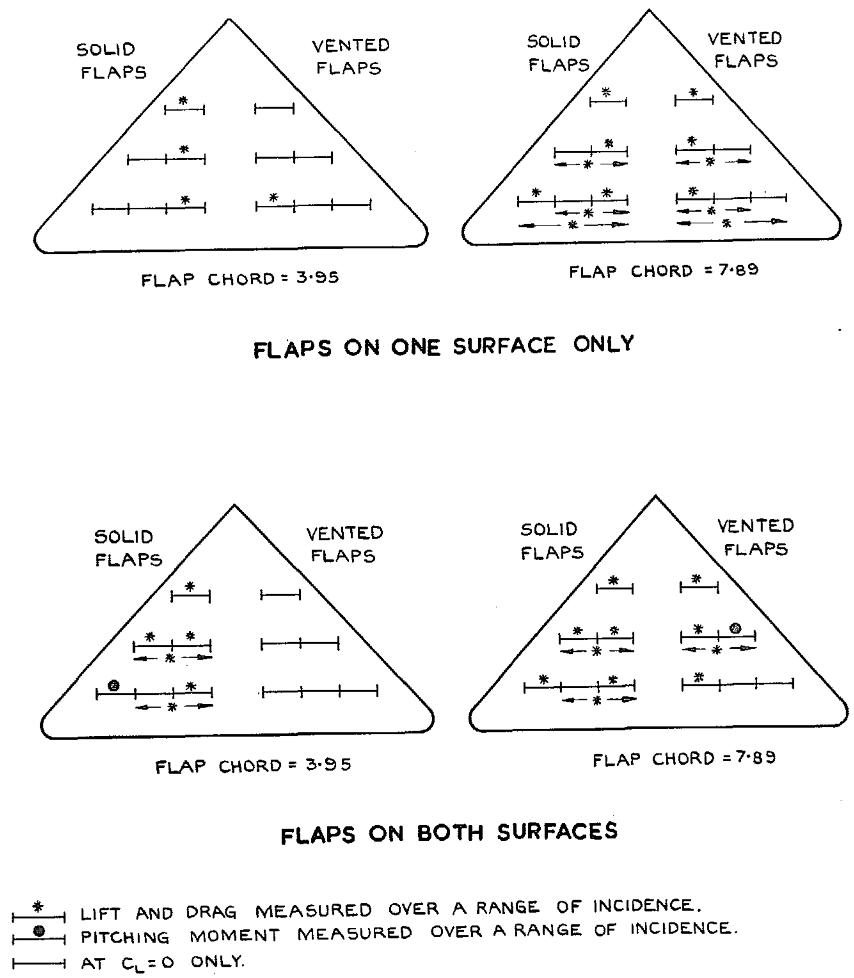

DIMENSIONS GIVEN AS PERCENT WING CENTRE LINE CHORD.

FIG. 2. Layout of tests.

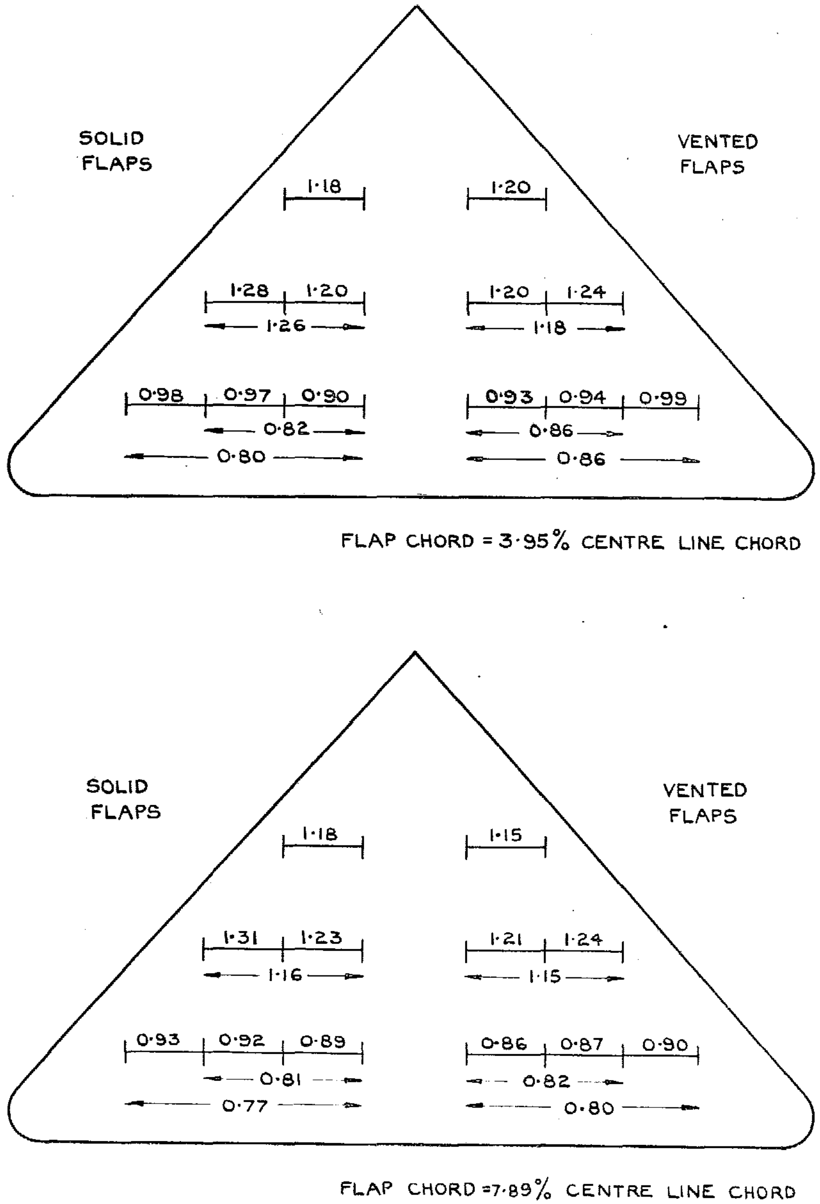

FIG. 3. Flap drag C_F at $C_L = 0$. One surface.

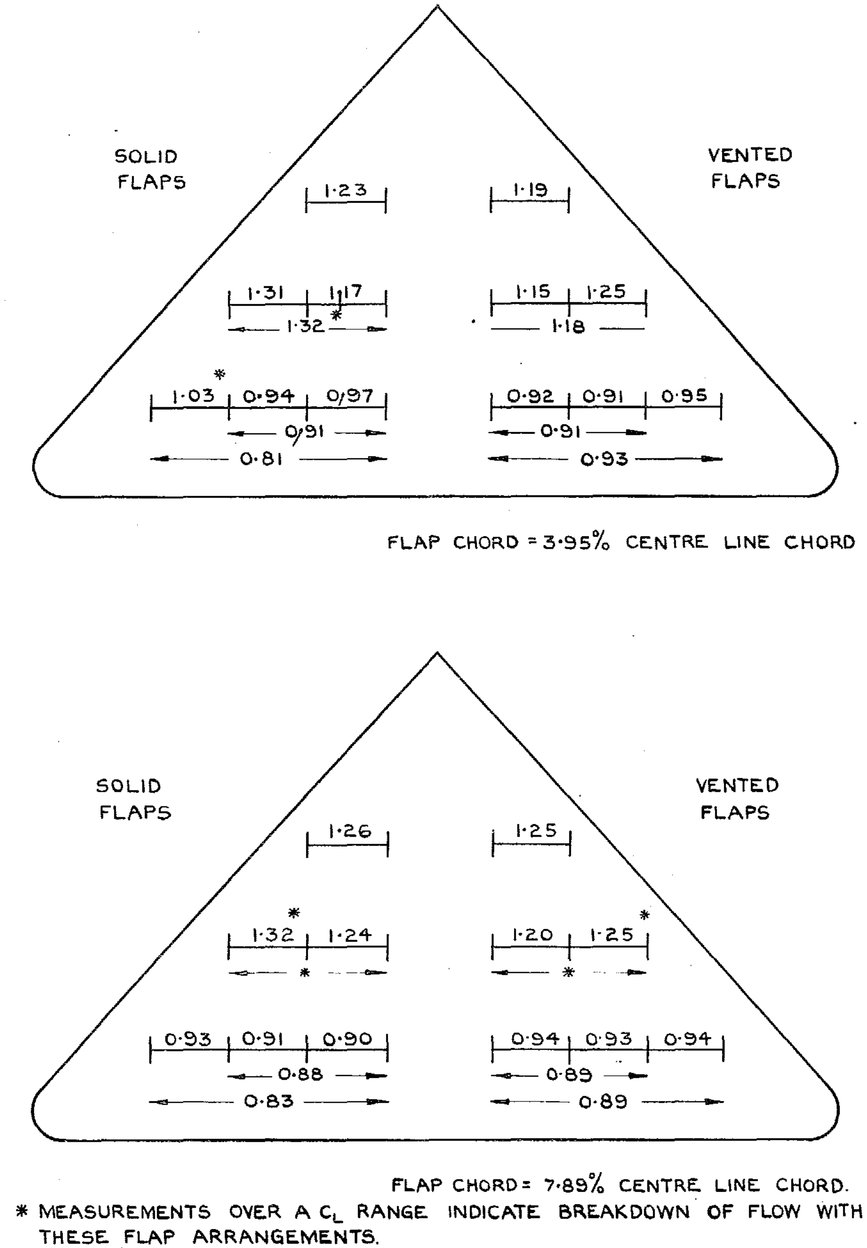

FIG. 4. Flap drag C_F at $C_L = 0$. Both surfaces.

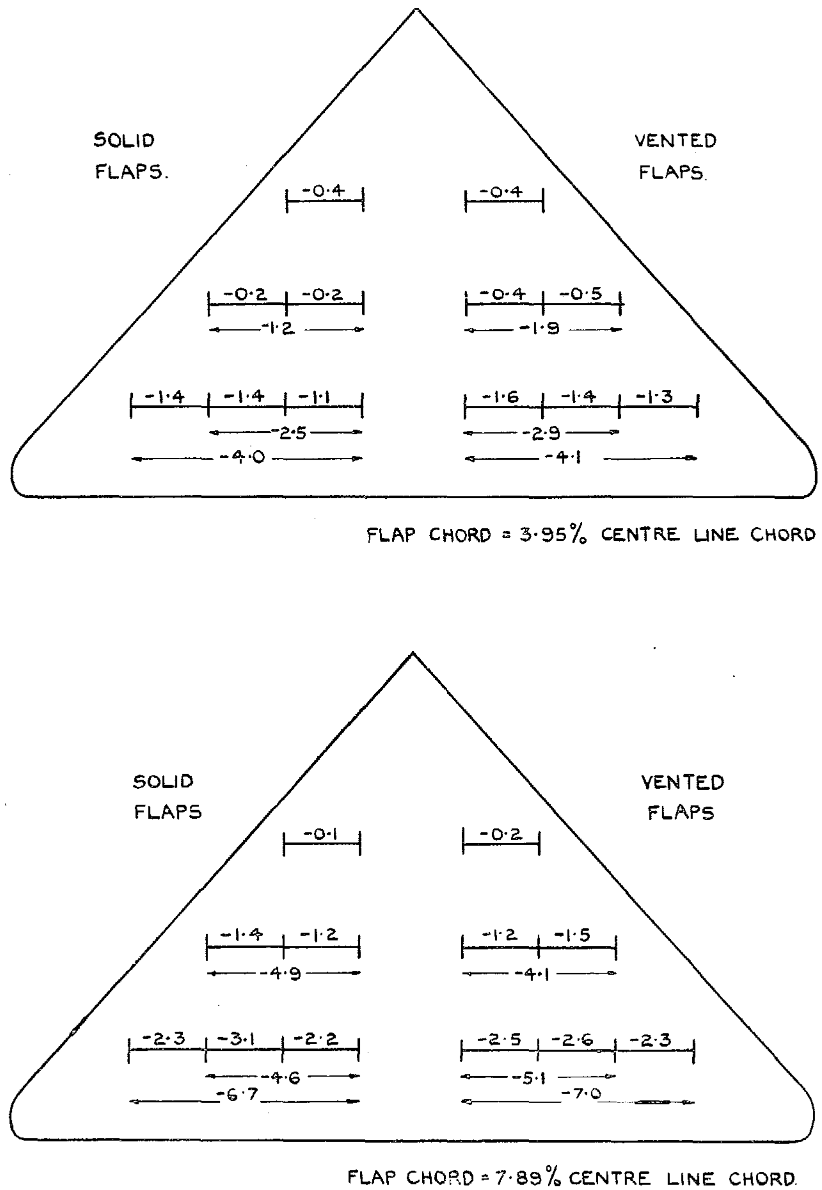

FIG. 5. Δ (no-lift angle) due to flaps (degrees). Lower surface.

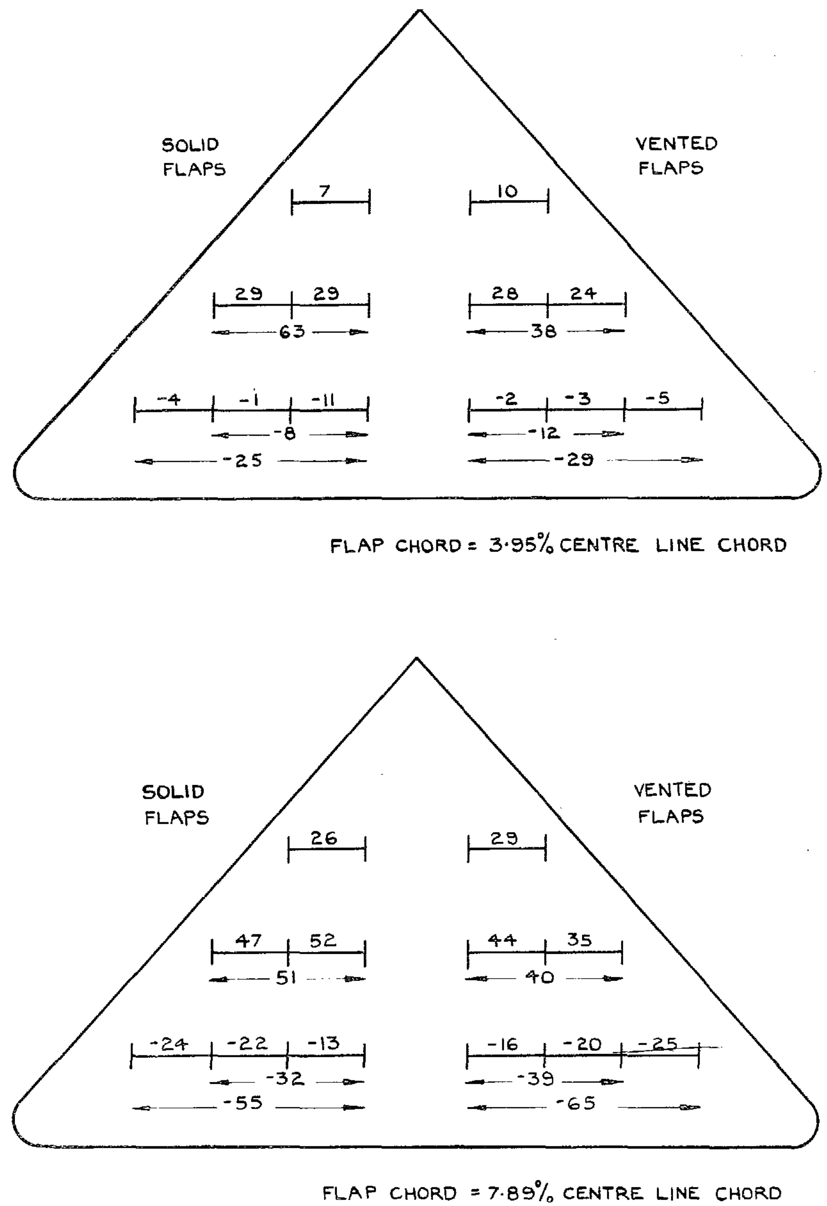

FIG. 6. $\Delta C_m \times 10^3$ due to flaps. $C_L = 0$. Lower surface.

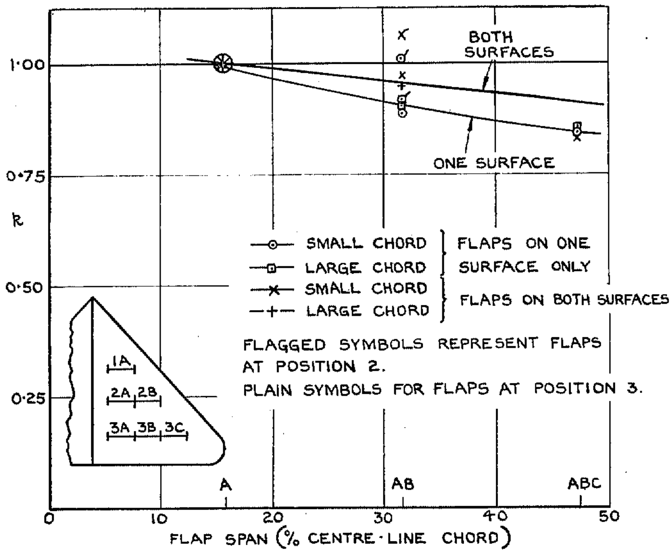

FIG. 7a. Solid flaps.

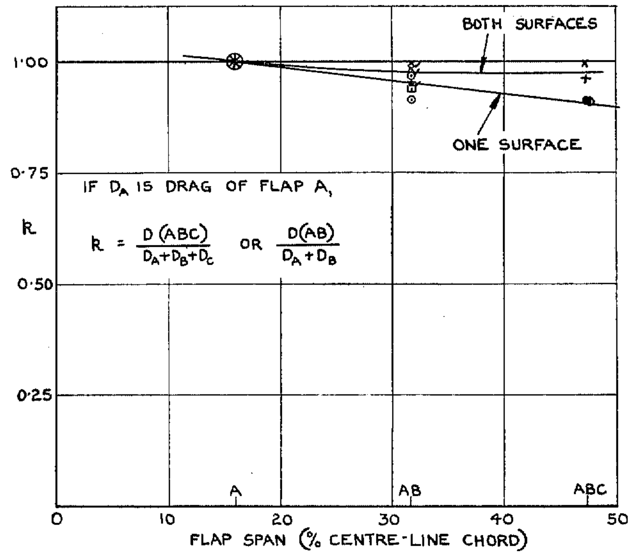

FIG. 7b. Vented flaps.

FIGS. 7a and 7b. Effect of flap span on drag.

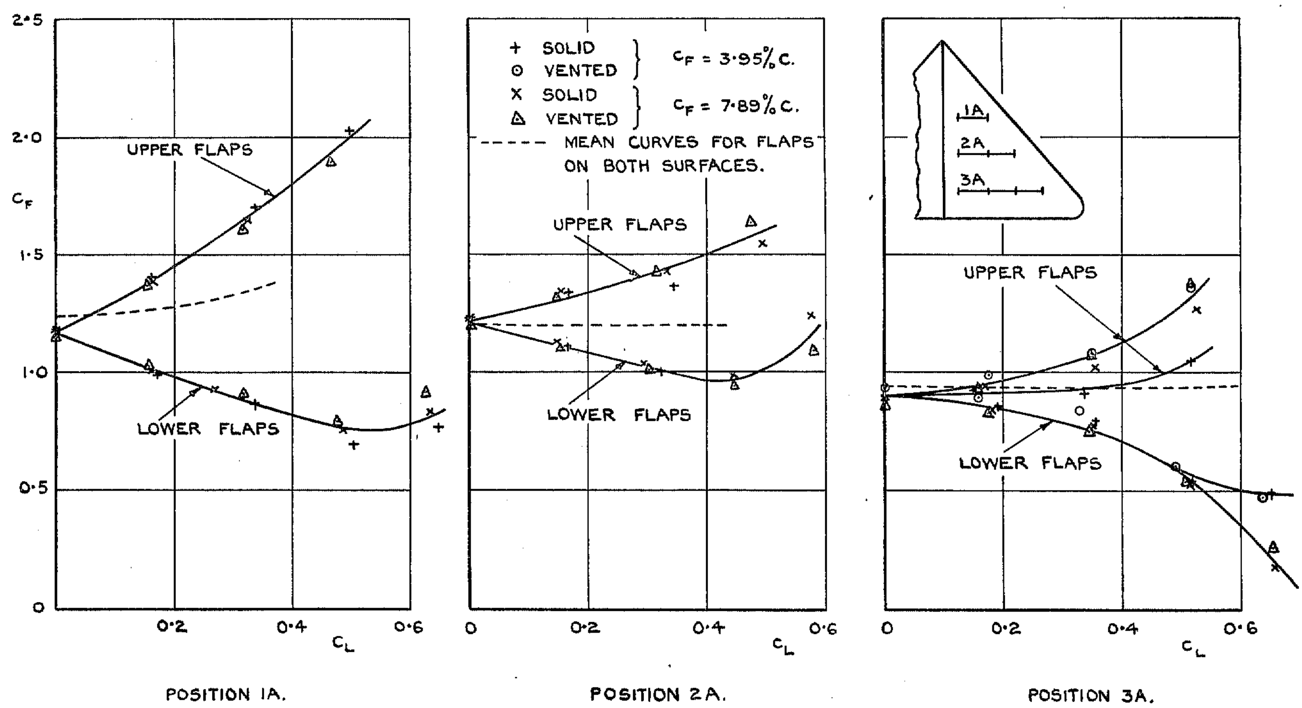

FIG. 8. Variation of flap drag with lift.

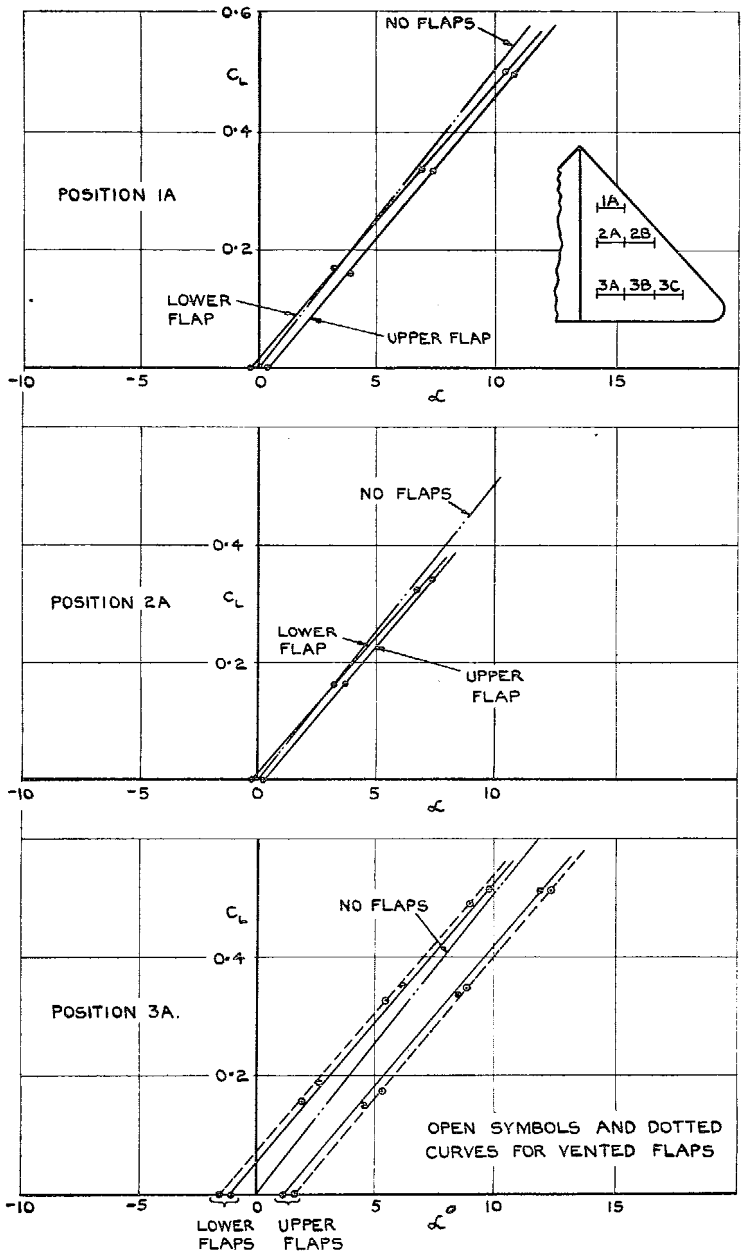

FIG. 9. Lift with brake flaps. One surface.
$C_F = 3{\cdot}95$ per cent C.

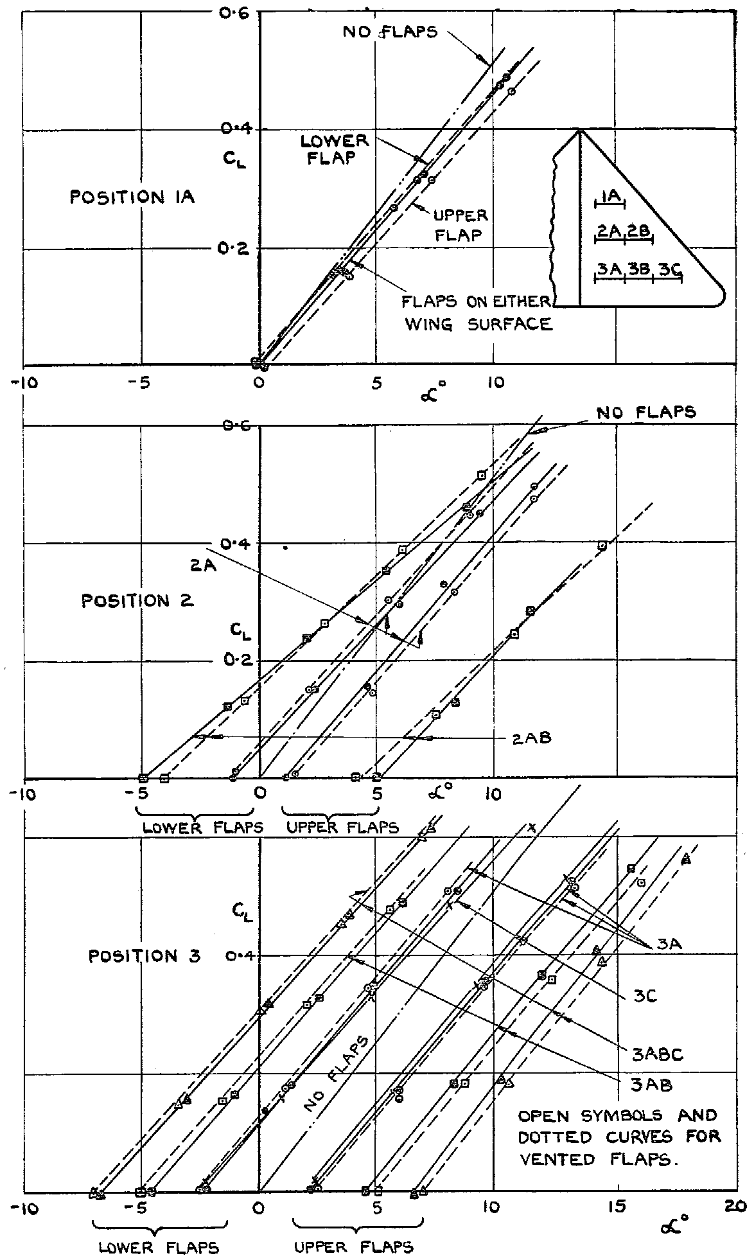

FIG. 10. Lift with brake flaps. One surface.
$C_F = 7{\cdot}69$ per cent C.

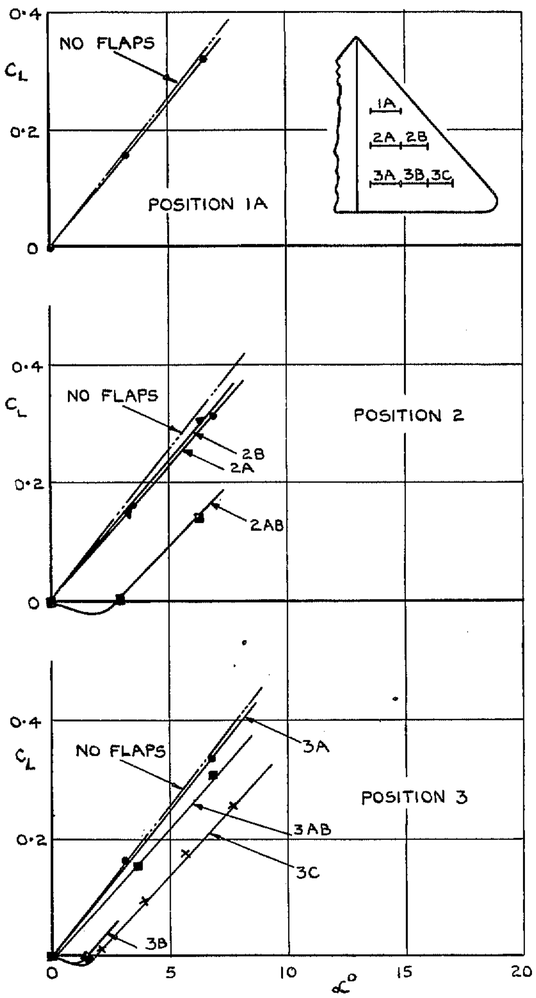

FIG. 11. Lift with brake flaps. Both surfaces. $C_F = 3{\cdot}95$ per cent C.

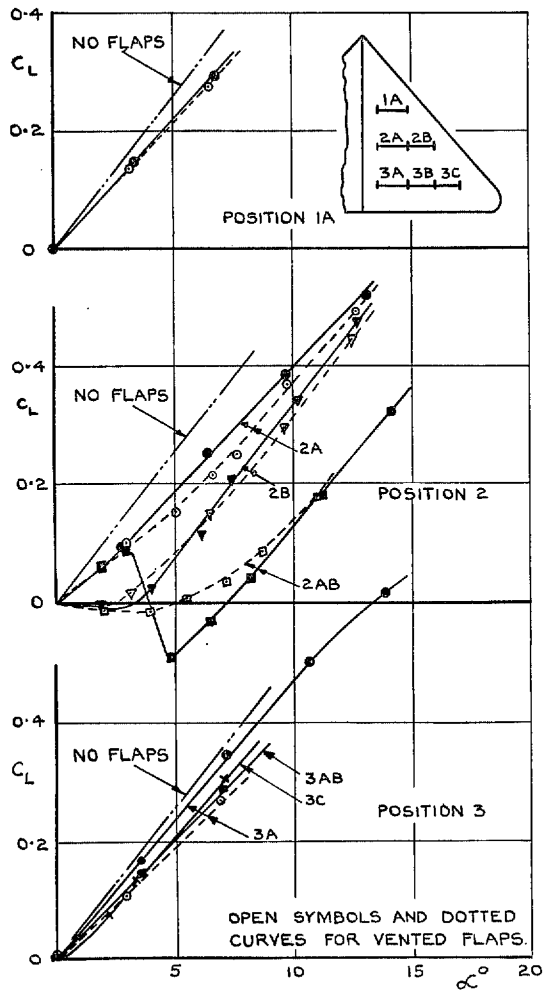

FIG. 12. Lift with brake flaps. Both surfaces. $C_F = 7{\cdot}89$ per cent C.

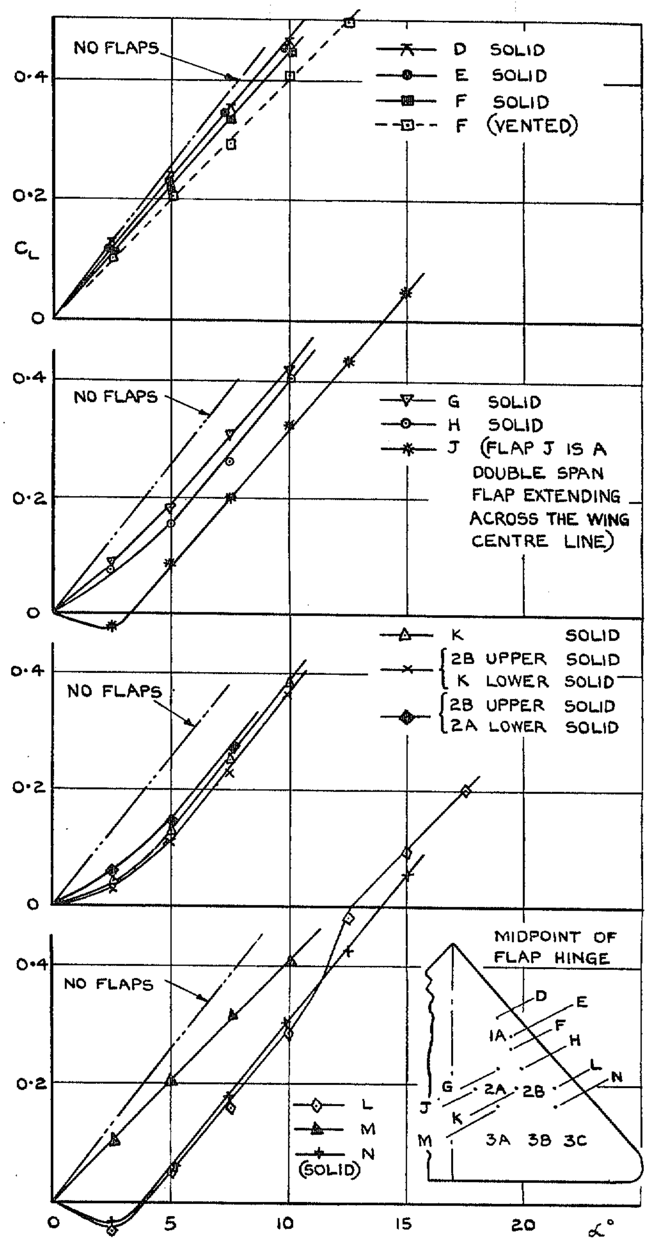

FIG. 13. Lift with brake flaps. Extra flap positions. $C_F = 7 \cdot 89$ per cent C. $b_F = 15 \cdot 8$ per cent C.

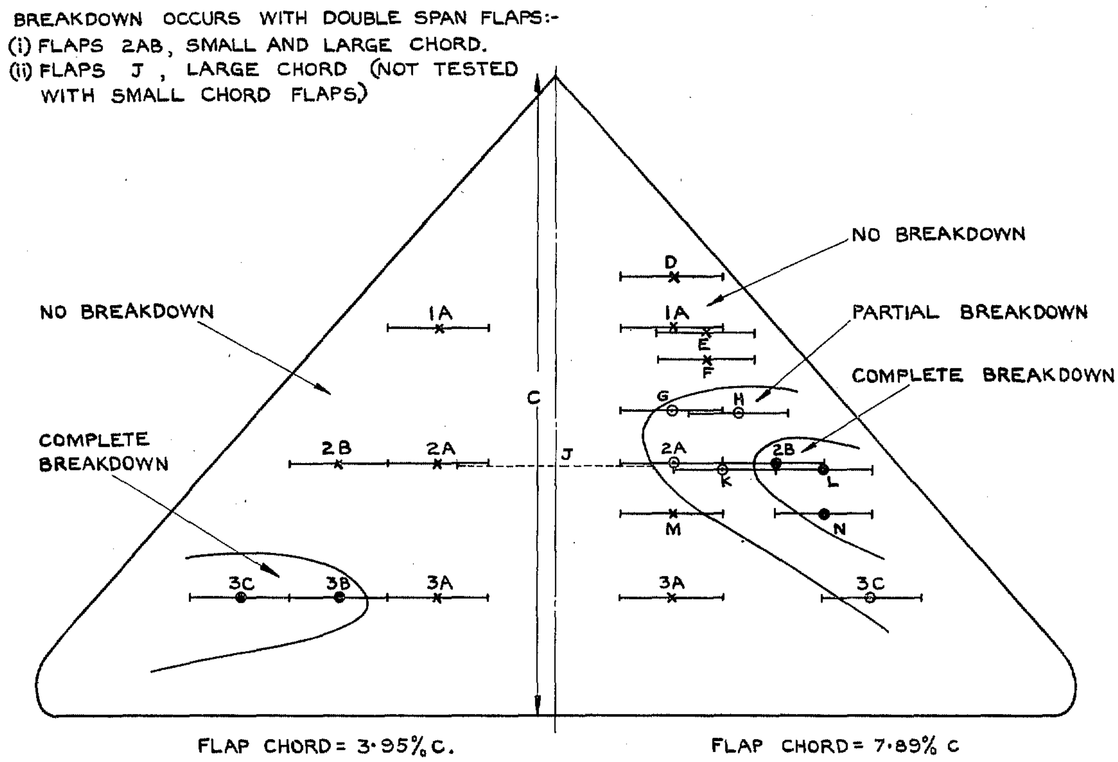

FIG. 14. Region in which solid flaps on both surfaces may cause breakdown of flow. $b_F = 15{\cdot}8$ per cent C. (Contours drawn for midpoint of flap hinge.)

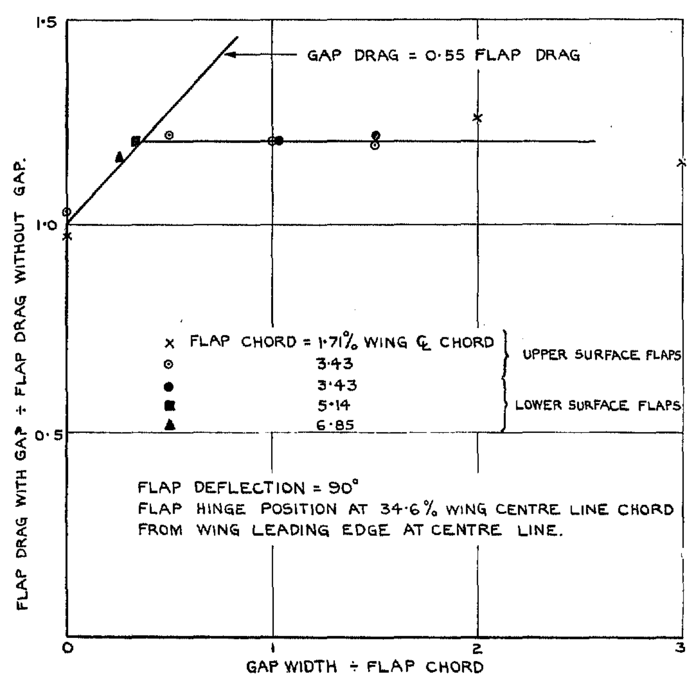

THE DRAG OF THE BRACKETS HAS BEEN SUBTRACTED FROM THE DRAG OF FLAP WITH GAP, ASSUMING THIS DRAG TO BE THE SAME PER UNIT AREA AS FOR THE FLAP.

FIG. 15. Effect of gap width on flap drag at $C_L = 0$.

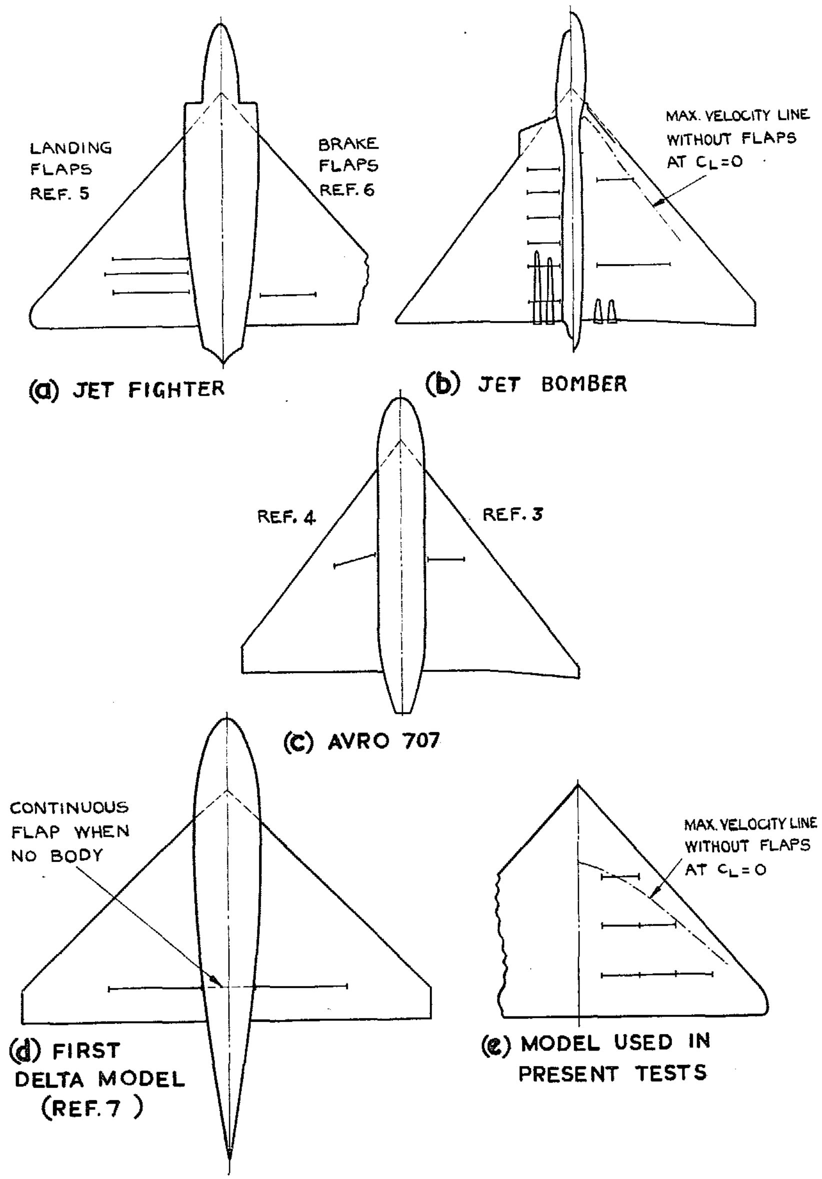

FIGS. 16a to 16e. Models from which brake flap drag data in Fig. 17 are taken.

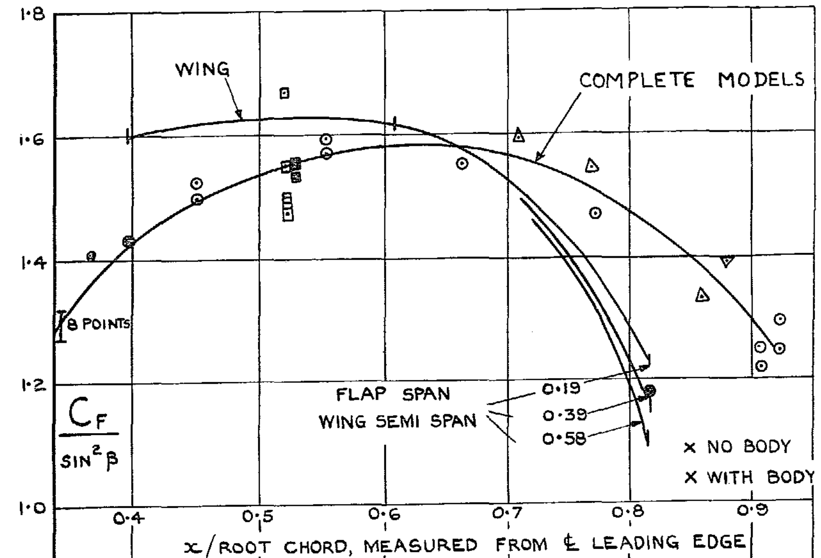

REF.	AIRCRAFT	SIGN	SECTION	LE SWEEP	% $\frac{C_F}{C}$	$\frac{g}{C_F}$	β°
	JET BOMBER	⊙	NACA 0010	52·4	3 TO 9	0 TO ½	30, 50, 60.
	"	I	NACA 0010	52·4	3½ TO 7	0 TO 1½	90
	"	⊛	NACA 0010	49·9	4	0	60
3	AVRO 707	⊡	NACA 0010	52·4	¾ TO 5	½ TO 5	60
4	AVRO 707	▣	NACA 0010	52·4	2½ TO 5	½ TO 1	75
5	JET FIGHTER	△	R.A.E. 102	48·5	7½ TO 14	0	40, 60
6	"	▽	R.A.E. 102	48·5	4½	0·1	60
7	FIRST DELTA MODEL	×	R.A.E. 102	45·0	15	0	60

ALL WINGS 10% THICK
C IS CENTRE-LINE CHORD.

FIG 17. Flap drag coefficient for 10 per cent thick deltas of about 50-deg sweep at $C_L = 0$.

PART II

The Effects of Flow Re-attachment Behind Split Flaps on a Delta Wing

1. *Introduction.*—It has been found in flight tests of a delta wing aircraft that the forward-mounted split flaps produced trim changes which were grossly non-linear with flap deflection. Wind-tunnel tests confirmed this, and also showed that for small flap deflections the flaps reduced the lift at constant incidence.

The existence of a region on a delta wing where flap behaviour is unusual has been noted in Part I. It was shown that in certain positions on the wing, single-surface brake flaps produced marked losses of lift slope resulting in negative lift increments at incidence with flaps on the lower surface (*see* Fig. 2). It was also shown that the effects of upper- and lower-surface flaps were sometimes additive (Fig. 2a) but sometimes caused a breakdown of flow resulting in negative overall lift slopes over a small range of incidence near zero lift (Fig. 2b). Both these effects were thought to be due to a re-attachment of flow to the wing surface behind the flap at some incidences but not at others. It was suggested that the occurrence of a flow of this sort depends on the relation between the chord of the flap and its distance from the trailing edge of the wing.

These phenomena are not peculiar to wings of delta plan-form, the breakdown of the lift curve with flaps on both surfaces having been found on unswept wings with brake flaps mounted well forward (Ref. 1).

In order to obtain some systematic data on this behaviour some model tests have been made on a delta wing with a range of lower-surface flaps and the results are presented here.

2. *Description of Tests.*—The model consisted of a 10 per cent thick delta wing and flaps of chord about 8 per cent wing centre-line chord which were used in Part I. The notation of Part I has been retained. The unit flap has a span of 16 per cent wing centre-line chord per side; its fore-and-aft position is designated by the numbers 1, 2, etc., where $3\frac{1}{2}$ refers to a trailing-edge flap, and its spanwise position by the letters A, B, etc., where A is nearest to the centre-line. The layout may be seen in Fig. 1 and dimensions are given in Table 1.

The following table shows the flap arrangements used, all being tested over a range of flap deflections up to 60 deg.

Spanwise position	Chordwise position	Flap aspect ratio
Double unit AB	$2, 2\frac{1}{2}, 3, 3\frac{1}{2}$	4
Double unit joined across the centre-line ABJ	$2, 2\frac{1}{2}$	10·7
Single unit A	$2\frac{1}{2}$	2

Measurements of lift, drag and pitching moment over the incidence range 0 to 8 deg were made, the pitching moments being quoted about an axis $0\cdot33\bar{c}$ aft of the leading edge of the standard mean chord (0·541 centre-line chord) instead of about $0\cdot25\bar{c}$ (0·498 centre-line chord) as in Part I. The tests were made in the Royal Aircraft Establishment 5-ft Wind Tunnel at a Reynolds number of $0\cdot67 \times 10^6$ based on the wing mean chord. One arrangement of flaps, $2\frac{1}{2}$AB deflected 25·5 deg, was tested at a Reynolds number of $1\cdot0 \times 10^6$ and showed no scale effect over this range.

3. *Discussion of Results.*—The results show that there are two types of behaviour:

(*a*) For all the flaps tested except those at the wing trailing edge, small flap deflections cause zero or negative lift increments (Fig. 3), positive pitching-moment increments (Fig. 4) and negligible changes in lift-curve slope (Fig. 5). Some tuft observations confirmed that this occurs when the flow breaking away from the flap trailing edge re-attaches to the wing surface behind the flap.

(*b*) For larger flap angles increasing flap deflection results in a positive lift increment, a negative pitching-moment increment and a loss of lift-curve slope depending on the chordwise position of the flap.

The tests on flaps $2\frac{1}{2}$AB show that the change from (*a*) to (*b*) is a fairly sharp one.

The range of flap angle for which the flow re-attaches increases as the flap is moved forward on the wing. Following the suggestion of Part I an attempt has been made to correlate the flap lift increments with the relation between *h*, the height of the flap trailing edge from the wing surface, and *l*, the distance of the flap trailing edge ahead of the wing trailing edge. Values at zero incidence of flap lift coefficient* C_{FL} per degree of flap angle are plotted against h/l in Fig. 6. Some results extracted from Part I are also included. This method of presentation enables a single curve to be drawn through all the results at a given flap span; which suggests that the chordwise position of the flap affects the lift only through its effect on h/l.

The effect of flap span shown in Fig. 6 may be due to its effect on flap aspect ratio or to the effect of spanwise position on the (delta) wing. Fig. 3 shows the flap lift increments at $\alpha = 0$ deg and at $\alpha = 8$ deg, and it will be seen that the critical flap angles are the same. This change in pressure distribution is larger than that due to spanwise movement of a flap at a given α, suggesting that the local wing pressure distribution does not effect the critical. To check the aspect ratio effect, some measurements with 4 per cent chord flaps (from Part I) have been used. These results are plotted in Fig. 7 together with the two curve 'flaps AB' and 'flaps A' from Fig. 6. The accuracy is bad due to the small size of the flaps but the points suggest a value of $(h/l)_{crit}$ nearer to 0·15 than to 0·2 and thus that the variation is with aspect ratio rather than with spanwise position. This critical value of (h/l) then varies with flap aspect ratio as shown in Fig. 8. A point extracted from some National Advisory Committee for Aeronautics tests on a two-dimensional wing of 65–210 section (Ref. 2) is also shown. This fits in well with the present results, indicating that the effect of wing plan-form is small. A point extracted from some model tests on a Delta wing fighter (Ref. 3) is also shown. This also agrees with the present results.

4. *Conclusions*.—(*a*) The results show that split flaps on the lower surface of a wing exhibit a critical value of the ratio of the height of the flap trailing edge from the wing surface (*h*) to its distance from the wing trailing edge (*l*).

(*b*) At values of h/l below this critical, the flow re-attaches to the wing surface behind the flap and this results in negative lift increments and positive pitching moments.

(*c*) The critical value of h/l varies with the aspect ratio of the flap. The critical obtained from some N.A.C.A. tests on a two-dimensional wing (Ref. 2) fits in well with the present results, indicating that the effect of wing plan-form is small, at any rate at large flap aspect ratio.

REFERENCES

No.	*Author*	*Title, etc.*
1	R. H. Whitby and F. J. Bigg ..	Wind-tunnel tests on the effect of brake flaps on lift and trim. R.A.E. Report Aero. 1744. A.R.C. 5860. March, 1942.
2	R. N. Olson and J. N. Benezra ..	High speed wind tunnel investigation of dive recovery flaps for lift control on the NACA 65–210 aerofoil. N.A.C.A./T.I.B./1090. A.R.R. 6D23. August, 1946.
3	J. W. Leathers and J. F. Holford..	R.A.E. Report Aero 2306b.

* Where $C_{FL} = \Delta C_L \times \dfrac{\text{Wing area}}{\text{Flap area}}$.

TABLE 1

Details of Wing and Flaps

All linear dimensions given as a percentage of the wing centre-line chord c

$c = 19 \cdot 0$ in.

Wing	
Area	$0 \cdot 889c^2$
Span	164·2
Mean chord	54·2
Aspect ratio	3·03
Section	RAE 101 (symmetrical)
Thickness/chord ratio	10 per cent at 31 per cent chord
Sweepback of leading edge	48 deg
Dihedral	0 deg
Twist	0 deg
Pitching-moment axis	
Aft of centre-line leading edge	54·1
Aft of leading edge of standard mean chord	$0 \cdot 33\bar{c}$
Flaps	
Chord $= c_F$	7·89
Chordwise position of hinge line—position 2	60·5
" 2½	71·1
" 3	81·6
" 3½	92·1
Span—flaps AB	2 × 31·6
ABJ	1 × 84·2
A	2 × 15·8
Deflection	0 to 60 deg

TABLE 2

Effect of Flaps at Constant Incidence

2 AB (hinge line at 0·605c)

δ_F (deg)	α (deg)	ΔC_L	ΔC_D	ΔC_m
20	0	−0·007	0·0148	0·0206
	2	−0·007	0·0142	0·0194
	4	−0·008	0·0136	0·0181
	6	−0·009	0·0132	0·0168
	8	−0·009	0·0119	0·0140
40	0	+0·028	0·0415	0·0632
	2	+0·012	0·0399	0·0624
	4	−0·004	0·0375	0·0615
	6	−0·020	0·0347	0·0605
	8	−0·036	0·0310	0·0567
60	0	0·146	0·0624	0·0571
	2	0·115	0·0620	0·0601
	4	0·083	0·0602	0·0631
	6	0·051	0·0578	0·0662
	8	0·020	0·0548	0·0708

2½ AB (hinge line at 0·711c)

δ_F (deg)	α (deg)	ΔC_L	ΔC_D	ΔC_m
20	0	−0·007	0·0130	0·0223
	2	−0·007	0·0127	0·0211
	4	−0·008	0·0123	0·0197
	6	−0·009	0·0121	0·0184
	8	−0·009	0·0111	0·0188
24	0	+0·003	0·0165	0·0311
	2	−0·005	0·0158	0·0312
	4	−0·012	0·0149	0·0314
	6	−0·019	0·0135	0·0320
	8	−0·027	0·0123	0·0322
25·5	0	+0·008	0·0176	0·0311
	2	0	0·0172	0·0315
	4	−0·007	0·0163	0·0318
	6	−0·014	0·0149	0·0324
	8	−0·022	0·0140	0·0333
30	0	0·045	0·0228	0·0289
	2	0·035	0·0231	0·0293
	4	0·025	0·0229	0·0301
	6	0·015	0·0222	0·0315
	8	0·005	0·0213	0·0328
40	0	0·112	0·0356	0·0191
	2	0·101	0·0372	0·0197
	4	0·089	0·0381	0·0201
	6	0·077	0·0391	0·0206
	8	0·066	0·0400	0·0228
60	0	0·210	0·0554	0·0078
	2	0·195	0·0582	0·0079
	4	0·180	0·0605	0·0078
	6	0·165	0·0629	0·0078
	8	0·150	0·0672	0·0095

TABLE 2—*continued*

3 AB (hinge line at 0·816*c*)

δ_F (deg)	α (deg)	ΔC_L	ΔC_D	ΔC_m
20	0	0·053	0·0109	−0·0029
	2	0·051	0·0123	−0·0041
	4	0·050	0·0137	−0·0044
	6	0·049	0·0151	−0·0040
	8	0·047	0·0163	−0·0032
40	0	0·171	0·0300	−0·0294
	2	0·167	0·0340	−0·0305
	4	0·162	0·0377	−0·0308
	6	0·157	0·0414	−0·0303
	8	0·153	0·0463	−0·0295
60	0	0·248	0·0504	−0·0399
	2	0·243	0·0556	−0·0413
	4	0·237	0·0608	−0·0418
	6	0·231	0·0662	−0·0416
	8	0·226	0·0739	−0·0411

3½ AB (hinge line at 0·921*c*)

δ_F (deg)	α (deg)	ΔC_L	ΔC_D	ΔC_m
20	0	0·099	0·0100	−0·0381
	2	0·103	0·0127	−0·0399
	4	0·107	0·0154	−0·0422
	6	0·111	0·0182	−0·0441
	8	0·115	0·0232	−0·0456
40	0	0·196	0·0284	−0·0716
	2	0·200	0·0338	−0·0740
	4	0·204	0·0389	−0·0768
	6	0·208	0·0445	−0·0792
	8	0·212	0·0541	−0·0811
60	0	0·275	0·0493	−0·0921
	2	0·277	0·0564	−0·0949
	4	0·280	0·0634	−0·0981
	6	0·283	0·0711	−0·1003
	8	0·285	0·0839	−0·1018

2 ABJ (hinge line at 0·605*c*)

δ_F (deg)	α (deg)	ΔC_L	ΔC_D	ΔC_m
12·5	0	−0·013	0·0079	0·0152
	2	−0·013	0·0075	0·0127
	4	−0·012	0·0070	0·0109
	6	−0·011	0·0067	0·0099
	8	−0·011	0·0066	0·0095
24	0	+0·006	0·0254	0·0470
	2	+0·001	0·0243	0·0452
	4	−0·005	0·0230	0·0431
	6	−0·011	0·0213	0·0410
	8	−0·016	0·0200	0·0395
40	0	0·127	0·0521	0·0496
	2	0·107	0·0524	0·0507
	4	0·088	0·0521	0·0516
	6	0·069	0·0509	0·0532
	8	0·049	0·0506	0·0546
60	0	0·219	0·0779	0·0481
	2	0·193	0·0790	0·0490
	4	0·167	0·0790	0·0506
	6	0·141	0·0789	0·0531
	8	0·115	0·0815	0·0573

2½ ABJ (hinge line at 0·711*c*)

δ_F (deg)	α (deg)	ΔC_L	ΔC_D	ΔC_m
11·5	0	−0·018	0·0066	0·0201
	2	−0·019	0·0061	0·0182
	4	−0·019	0·0055	0·0166
	6	−0·019	0·0050	0·0159
	8	−0·020	0·0046	0·0157
20·5	0	0·046	0·0170	0·0226
	2	0·039	0·0178	0·0227
	4	0·033	0·0180	0·0230
	6	0·027	0·0179	0·0242
	8	0·020	0·0184	0·0259
40	0	0·163	0·0411	0·0105
	2	0·152	0·0438	0·0110
	4	0·141	0·0462	0·0121
	6	0·130	0·0482	0·0141
	8	0·119	0·0519	0·0167
60	0	0·235	0·0711	0·0119
	2	0·221	0·0739	0·0114
	4	0·208	0·0769	0·0119
	6	0·195	0·0807	0·0137
	8	0·181	0·0867	0·0167

TABLE 2—*continued*

2½ A (hinge line at 0·711c)				
δ_F (deg)	α (deg)	ΔC_L	ΔC_D	ΔC_m
24	0	—0·011	0·0081	0·0129
	2	—0·011	0·0079	0·0105
	4	—0·011	0·0075	0·0086
	6	—0·011	0·0069	0·0071
	8	—0·011	0·0074	0·0054
40	0	+0·017	0·0177	0·0256
	2	0·013	0·0178	0·0253
	4	0·008	0·0173	0·0248
	6	+0·003	0·0166	0·0247
	8	—0·001	0·0166	0·0250
60	0	0·090	0·0290	0·0201
	2	0·083	0·0302	0·0191
	4	0·077	0·0309	0·0187
	6	0·071	0·0315	0·0191
	8	0·064	0·0327	0·0202

TABLE 3

Basic Wing Characteristics

α (deg)	C_L	C_D	C_m
0	0	0·0080	—0·0015
2	0·100	0·0104	—0·0020
4	0·200	0·0152	—0·0031
6	0·300	0·0227	—0·0051
8	0·400	0·0348	—0·0077

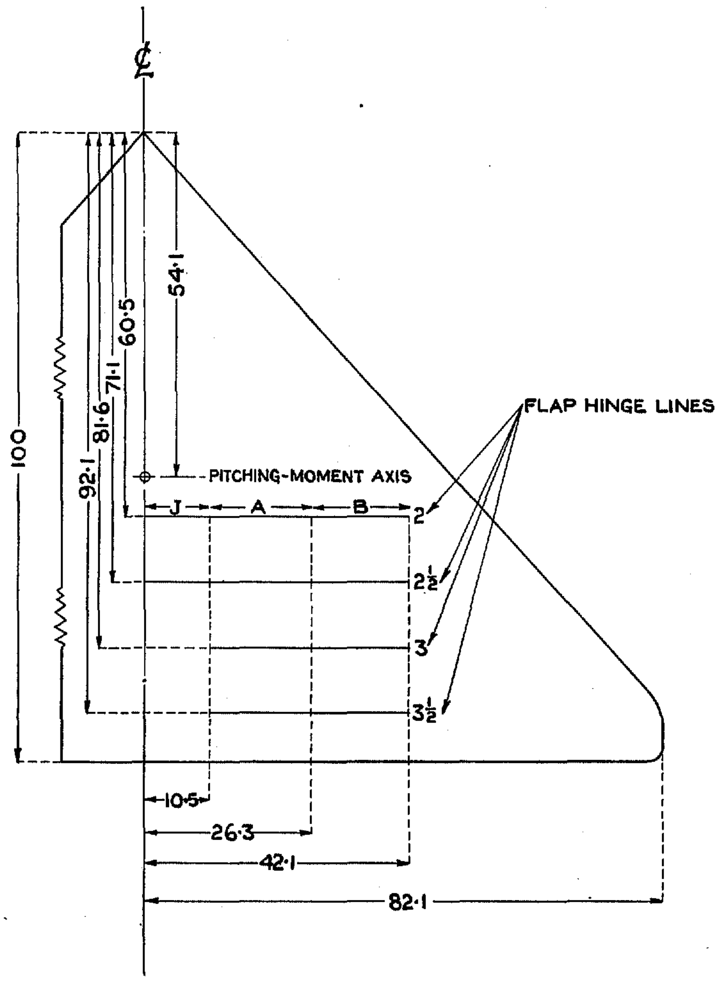

DIMENSIONS GIVEN AS PERCENT WING CENTRE-LINE CHORD

FIG. 1. Wing and flaps.

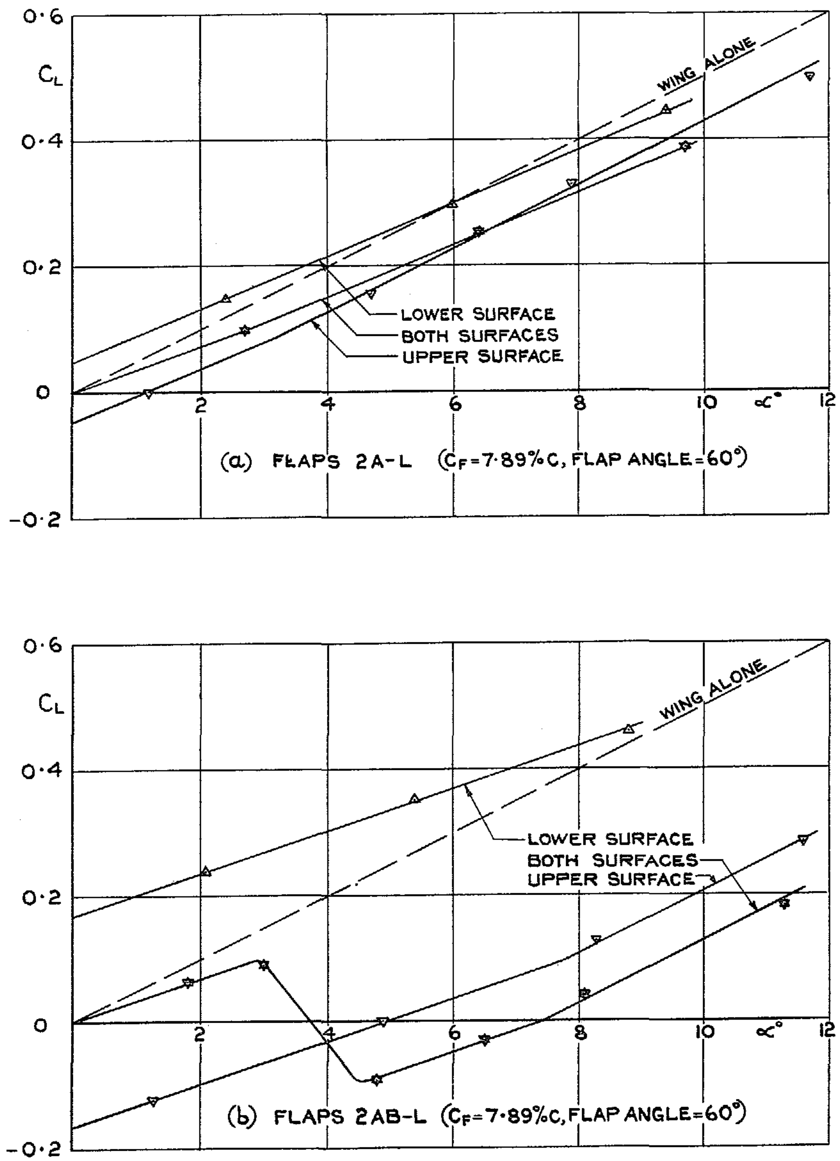

FIG. 2. Example of unusual flap behaviour (from Part I).

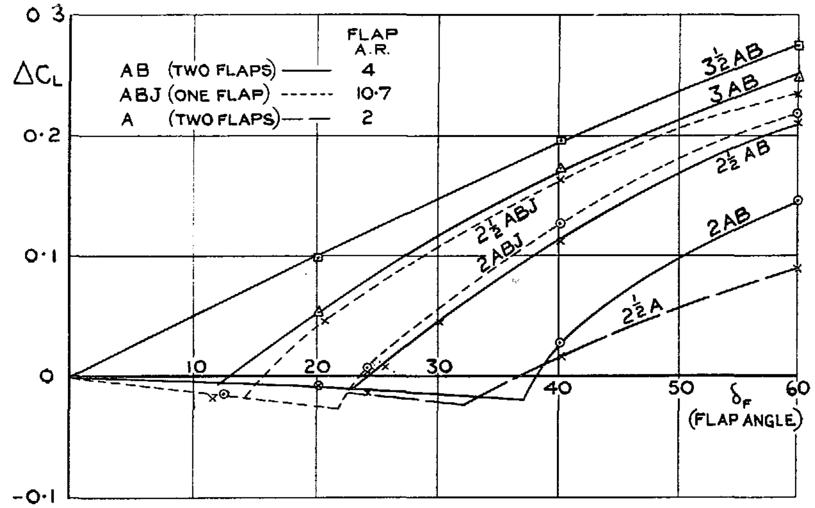

FIG. 3a. Flap lift increment at $\alpha = 0$ deg.

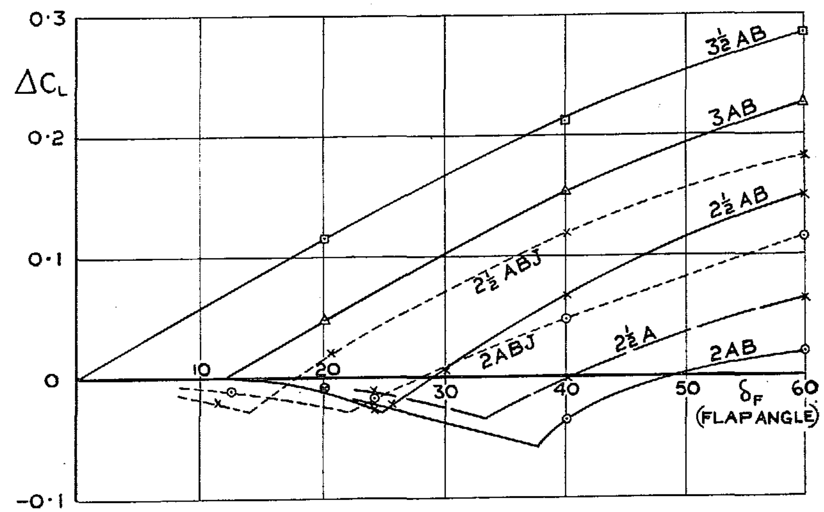

FIG. 3b. Flap lift increment at $\alpha = 8$ deg.

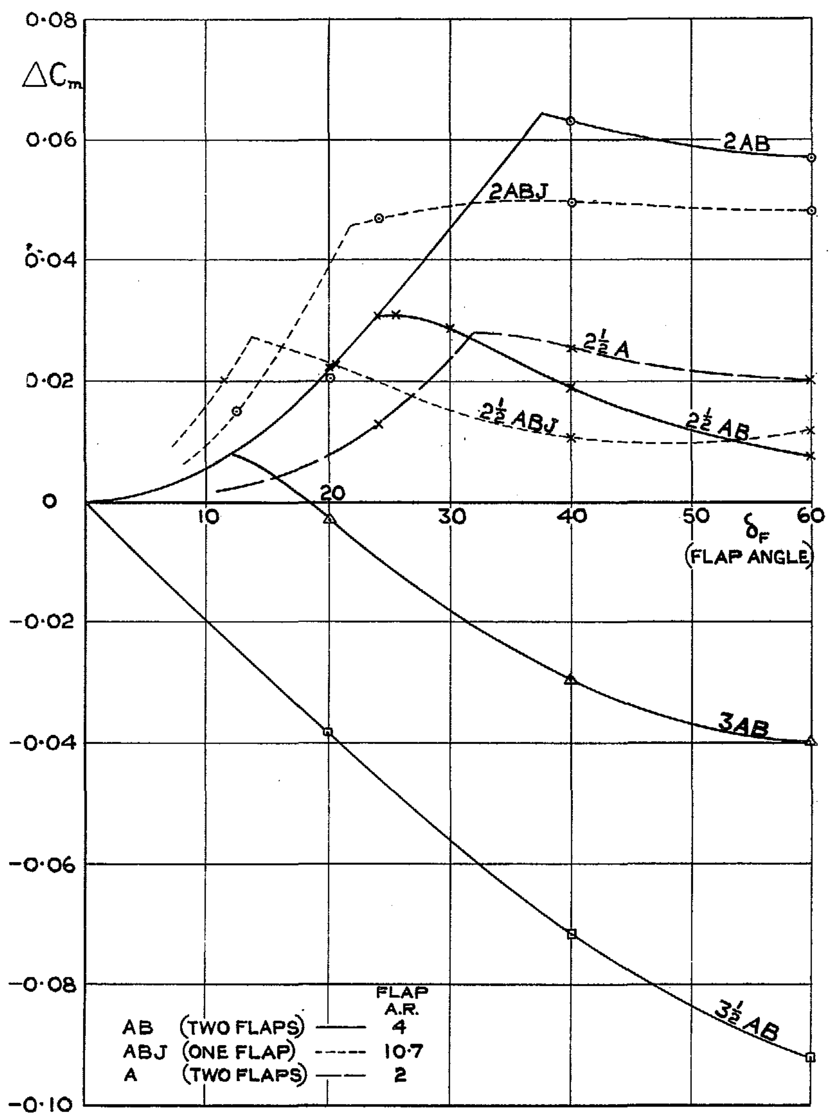

FIG. 4. Pitching moment due to flaps at $\alpha = 0$ deg.

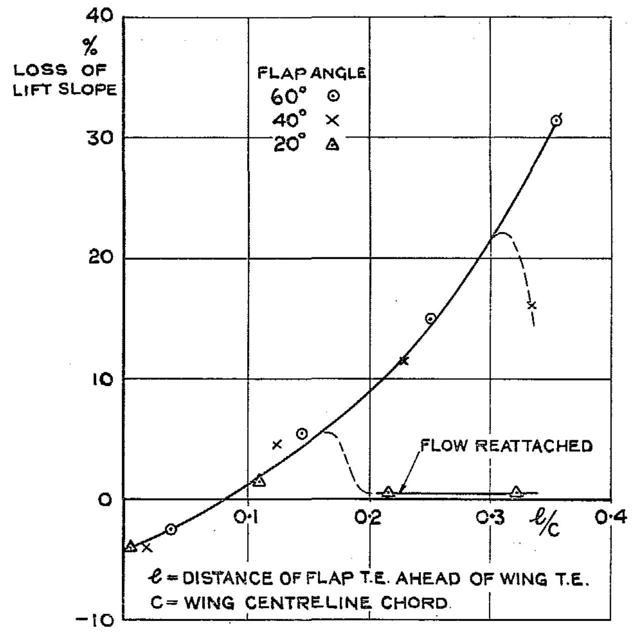

FIG. 5a. Variation of lift slope with chordwise position of flap AB.

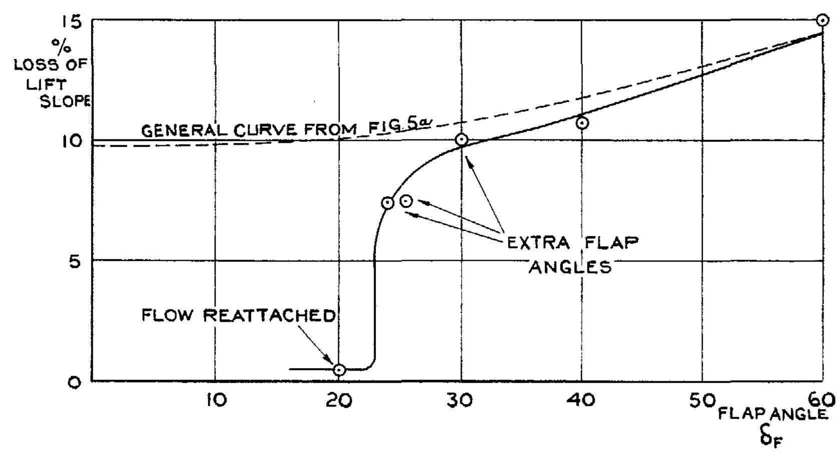

FIG. 5b. Variation of lift slope with flap angle for flap $2\frac{1}{2}$ AB.

(4966) Wt. 20/9036 K.7 3/57 H.W.

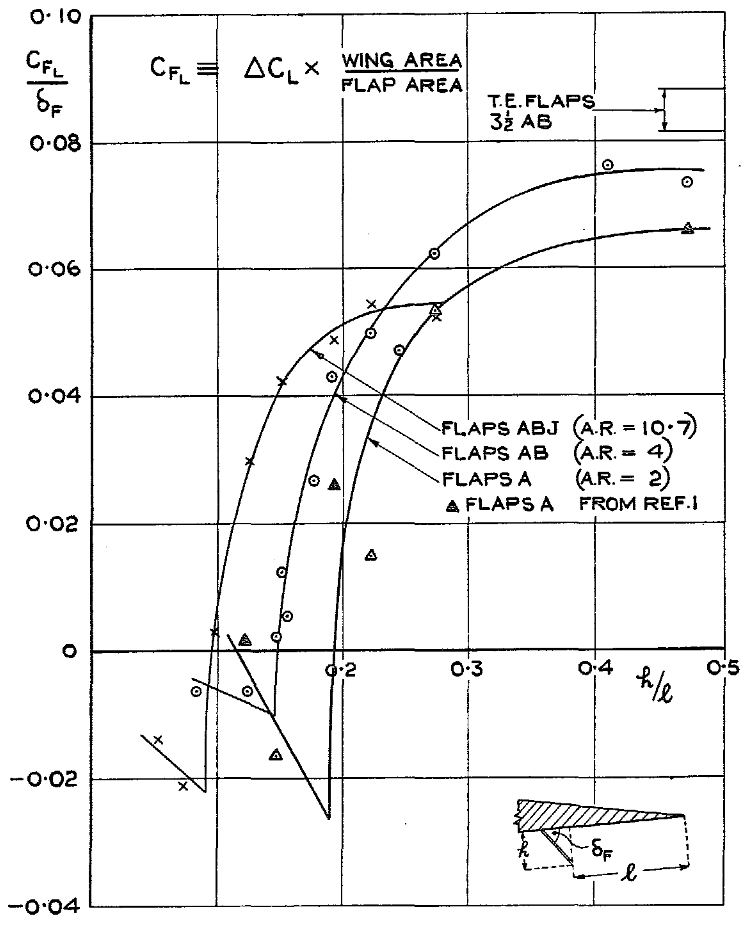

Fig. 6. Correlation of flap lift with position of flap trailing edge. $\alpha = 0$ deg.

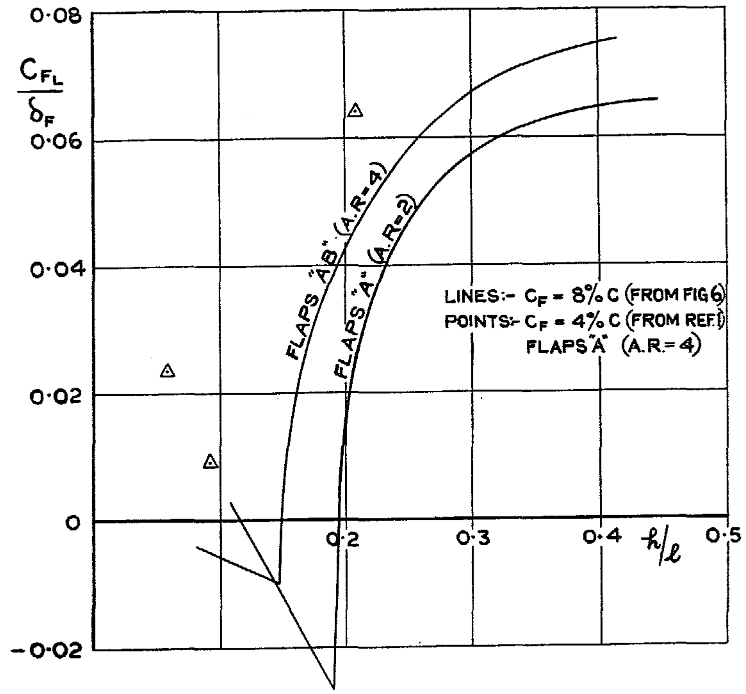

Fig. 7. Effect of flap chord on lift. $\alpha = 0$ deg.

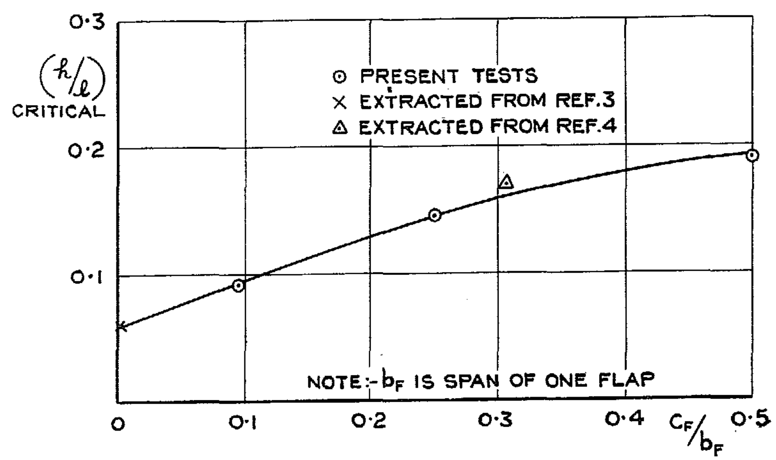

Fig. 8. Variation of critical value of h/l with flap aspect ratio.

PRINTED IN GREAT BRITAIN

Publications of the Aeronautical Research Council

ANNUAL TECHNICAL REPORTS OF THE AERONAUTICAL RESEARCH COUNCIL (BOUND VOLUMES)

1939 Vol. I. Aerodynamics General, Performance, Airscrews, Engines. 50s. (51s. 9d.)
Vol. II. Stability and Control, Flutter and Vibration, Instruments, Structures, Seaplanes, etc. 63s. (64s. 9d.)

1940 Aero and Hydrodynamics, Aerofoils, Airscrews, Engines, Flutter, Icing, Stability and Control Structures, and a miscellaneous section. 50s. (51s. 9d.)

1941 Aero and Hydrodynamics, Aerofoils, Airscrews, Engines, Flutter, Stability and Control Structures. 63s. (64s. 9d.)

1942 Vol. I. Aero and Hydrodynamics, Aerofoils, Airscrews, Engines. 75s. (76s. 9d.)
Vol II. Noise, Parachutes, Stability and Control, Structures, Vibration, Wind Tunnels. 47s. 6d. (49s. 3d.)

1943 Vol. I. Aerodynamics, Aerofoils, Airscrews. 80s. (81s. 9d.)
Vol II. Engines, Flutter, Materials, Parachutes, Performance, Stability and Control, Structures. 90s. (92s. 6d.)

1944 Vol. I. Aero and Hydrodynamics, Aerofoils, Aircraft, Airscrews, Controls. 84s. (86s. 3d.)
Vol. II. Flutter and Vibration, Materials, Miscellaneous, Navigation, Parachutes, Performance, Plates and Panels, Stability, Structures, Test Equipment, Wind Tunnels. 84s. (86s. 3d.)

1945 Vol. I. Aero and Hydrodynamics, Aerofoils. 130s. (132s. 6d.)
Vol. II. Aircraft, Airscrews, Controls. 130s. (132s. 6d.)
Vol. III. Flutter and Vibration, Instruments, Miscellaneous, Parachutes, Plates and Panels, Propulsion. 130s. (132s. 3d.)
Vol. IV. Stability, Structures, Wind Tunnels, Wind Tunnel Technique. 130s. (132s. 3d.)

Annual Reports of the Aeronautical Research Council—

1937 2s. (2s. 2d.) 1938 1s. 6d. (1s. 8d.) 1939–48 3s. (3s. 3d.)

Index to all Reports and Memoranda published in the Annual Technical Reports, and separately—

April, 1950 - - - - R. & M. 2600 2s. 6d. (2s. 8d.)

Author Index to all Reports and Memoranda of the Aeronautical Research Council—

1909—January, 1954 R. & M. No. 2570 15s. (15s. 6d.)

Indexes to the Technical Reports of the Aeronautical Research Council—

December 1, 1936—June 30, 1939	R. & M. No. 1850	1s. 3d. (1s. 5d.)
July 1, 1939—June 30, 1945	R. & M. No. 1950	1s. (1s. 2d.)
July 1, 1945—June 30, 1946	R. & M. No. 2050	1s. (1s. 2d.)
July 1, 1946—December 31, 1946	R. & M. No. 2150	1s. 3d. (1s. 5d.)
January 1, 1947—June 30, 1947	R. & M. No. 2250	1s. 3d. (1s. 5d.)

Published Reports and Memoranda of the Aeronautical Research Council—

Between Nos. 2251–2349	R. & M. No. 2350	1s. 9d. (1s. 11d.)
Between Nos. 2351–2449	R. & M. No. 2450	2s. (2s. 2d.)
Between Nos 2451–2549	R. & M. No. 2550	2s. 6d. (2s. 8d.)
Between Nos. 2551–2649	R. & M. No. 2650	2s. 6d. (2s. 8d.)

Prices in brackets include postage

HER MAJESTY'S STATIONERY OFFICE

York House, Kingsway, London W.C.2; 423 Oxford Street, London W.1 (Post Orders: P.O. Box 569, London S.E.1) 13a Castle Street, Edinburgh 2; 39 King Street, Manchester 2; 2 Edmund Street, Birmingham 3; 109 St. Mary Street, Cardiff; Tower Lane, Bristol, 1; 80 Chichester Street, Belfast, *or through any bookseller.*

S.O. Code No. 23-2996

R. & M. No. 2996